

## Tijdschrift van het NERG

Correspondentie-adres: postbus 39, 2260 AA Leidschendam. Internet: [www.nerg.nl](http://www.nerg.nl), secretariaat@nerg.nl  
Gironummer 94746 t.n.v. Penningmeester NERG, Leidschendam.

### DE VERENIGING NERG

Het NERG is een wetenschappelijke vereniging die zich ten doel stelt de kennis en het wetenschappelijk onderzoek op het gebied van de elektronica, signaalbewerking, communicatie- en informatietechnologie te bevorderen en de verbreiding en toepassing van die kennis te stimuleren.

### BESTUUR

prof.dr.ir. N.H.G. Baken, voorzitter  
prof.dr.ir. P. Regtien,  
vice-voorzitter  
ir. E. Bottelier, secretaris  
ir. J.G. van Hezewijk, penningmeester  
ir. H.J. Visser, tijdschrift-manager  
ir. B. Dunnebier,  
programma-manager  
ir. R.J. Kopmeiners, web-beheer  
ir. F. Speelman,  
onderwijs-commissaris  
vacature, ledenwervings-manager

### LIDMAATSCHAP

Voor het lidmaatschap wende men zich via het correspondentie-adres tot de secretaris of via de NERG website: <http://www.nerg.nl>. Het lidmaatschap van het NERG staat open voor hen, die aan een universiteit of hogeschool zijn afgestudeerd en die door hun kennis en ervaring bij kunnen dragen aan het NERG. De contributie wordt geheven per kalenderjaar en is inclusief abonnement op het Tijdschrift van het NERG en deelname aan vergaderingen, lezingen en excursies.

De jaarlijkse contributie bedraagt voor gewone leden € 43,- en voor studentleden € 21,50. Bij automatische incasso wordt € 2,- korting verleend. Gevorderde studenten aan een

universiteit of hogeschool komen in aanmerking voor het studentlidmaatschap. In bepaalde gevallen kunnen ook andere leden, na overleg met de penningmeester voor een gereduceerde contributie in aanmerking komen.

### HET TIJDSCHRIFT

Het tijdschrift verschijnt vijf maal per jaar. Opgenomen worden artikelen op het gebied van de elektronica, signaalbewerking, communicatie- en informatietechnologie. Auteurs, die publicatie van hun onderzoek in het tijdschrift overwegen, wordt verzocht vroegtijdig contact op te nemen met de hoofdredacteur of een lid van de Tijdschriftcommissie.

Voor toestemming tot overnemen van (delen van) artikelen dient men zich te wenden tot de tijdschriftcommissie. Alle rechten berusten bij de auteur tenzij anders vermeld.

### TIJDSCHRIFTCOMMISSIE

ir. H.J. Visser, voorzitter.  
TNO , Postbus 6235,  
5600 HE Eindhoven,  
E-mail: Visser@ieee.org  
ir. M. Arts, hoofdredacteur.  
ASTRON, Dwingeloo  
E-mail: Arts@astron.nl  
ir. G.W. Kant, redactielid.  
ASTRON, Dwingeloo,  
E-mail: kant@astron.nl  
ir. W.C. de Waard, redactielid.  
TNO, Postbus 5050,  
2600 GB Delft,  
E-mail: william.dewaard@tno.nl



### INHOUD

Van de redactie . . . . .	30
<i>Michel Arts</i>	
EMF and health - state of the science. . . . .	31
<i>Eric van Rongen, PhD</i>	
Blootstelling aan elektromagnetische straling tijdens MRI scanning . . . . .	38
<i>J. M. L. Engels</i>	
Software Defined Radio in reconfigurable logic . . . . .	44
<i>H.J.W. Medenblik, R.M.E.M van Heijster</i>	
Channelizer, The heart of ESM, ECM and SDR . . . . .	52
<i>van der Hoek</i>	
Software-Defined Radio Testbed for the Physical Layer of Wireless LANs . . . . .	54
<i>R. Schiphorst, N.A. Moseley and C.H. Slump</i>	
Spanningsversterking met weerstanden en condensatoren . . . . .	62
<i>Ir. H.C. Bleijerveld</i>	
Ledenmutaties NERG. . . . .	64
Herhaalde oproep voor leden van het NERG. . . . .	64



Deze uitgave van het NERG wordt geheel verzorgd door:

**Henk Visscher, Zutphen**

Advertenties: Henk Visscher

tel: (0575) 542380

E-mail: : [henk.v@wxs.nl](mailto:henk.v@wxs.nl)

ISSN 03743853

# Van de redactie

*Michel Arts*  
E-mail: arts@astron.nl



Dit inleidende stukje van uw hoofdredacteur begint zo langzamerhand een klaagzang te worden. Maar toch moet ik helaas een aantal negatieve ontwikkelingen constateren.

Ongeveer een jaar geleden leek alles nog in orde. Het aantal themabijeenkomsten was groot dus kopij voor ons tijdschrift leek geen probleem te zijn. Het blijkt echter moeilijk om sprekers van themabijeenkomsten zover te krijgen een artikel te laten schrijven naar aanleiding van hun bijdrage. Ook komt het voor dat toezeggingen voor artikelen niet (op tijd) nagekomen worden. Na het verschijnen van dit nummer is de redactie door haar kopij heen. Het enige dat we

voor de rest van dit jaar hebben is het verslag van de ALV, een artikel over de uitreiking van de Vederprijs met eventueel een bijdrage van de winnaar en het jaarlijks proefschriftenoverzicht. Hier kunnen we nog net een nummer mee vullen, maar daarna is de koek echt op.

Over de proefschriften kan ik wel een positieve ontwikkeling melden. De TU Delft geeft iedere maand een wetenschapsagenda uit die ook op internet staat. Deze bevat oa. een overzicht van alle promoties aan de TU Delft. Een jaaroverzicht van de relevante promoties is dus makkelijk te maken. In het laatste nummer van dit jaar zal de TU Delft dus

weer vermeld worden in het proefschriftenoverzicht.

In dit nummer staan, het begint een traditie te worden, weer twee themabijeenkomsten centraal namelijk "EM-velden in de maatschappij" en "software-defined radio".

Naast deze bijdragen is er een (kort) artikel van de heer Bleijerveld. Hij toont aan dat de spanningsoverdracht van RC-netwerken onder bepaalde omstandigheden groter kan zijn dan 1. Bij LC-netwerken is dit algemeen bekend (resonantie-opslingering) maar voor RC-netwerken is dit een minder bekend verschijnsel.



# EMF and health - state of the science

Eric van Rongen, PhD

Health Council of the Netherlands,

PO Box 16052, 2500 BB The Hague, The Netherlands,

e-mail eric.van.rongen@gr.nl



## Abstract

This paper gives a very short overview of a very broad field: studies into possible health effects of exposure to electromagnetic fields in the frequency range of 0 - 300 GHz. Different frequency ranges are discussed: static fields, extremely low frequency (powerline) fields and high frequency (radiofrequency) fields. An overview is given of which effects are considered scientifically established and which are not.

## Introduction

In the past decades, there has been an increase in the number of people that worry about possible health effects associated with exposure to electromagnetic fields. Alarming reports in the media and the growing number of visible sources of radiation, such as antennas for mobile telecommunication, contribute to this. Questions arise such as: Can I live safely near overhead power lines or will my child get cancer from that? Is my headache caused by the base station antenna on the rooftop of my apartment building? Can I get brain cancer if I use a cellular telephone?

Since the mid-1900's many studies have been done on possible health effects of exposure to electromagnetic fields. In the early 1990's, the focus was on exposure to powerline frequency fields (extremely low frequencies of 50 and 60 Hz). Towards the end of the century the focus shifted to radiofrequencies, particularly those used by mobile telecommunication systems (e.g. 900 and 1800 MHz for GSM).

Regularly the available scientific material is reviewed by international and national organizations, such as the International Commission on Nonionizing Radiation (ICNIRP) ([www.icnirp.de](http://www.icnirp.de)), the International Committee on Electromagnetic Safety (ICES) of the USA-based IEEE

(<http://grouper.ieee.org/groups/scc28/index.html>), the National Radiological Protection Board (NRPB) of the UK ([www.nrpb.org](http://www.nrpb.org)) and the Health Council of the Netherlands ([www.gr.nl](http://www.gr.nl)). The World Health Organization (WHO) runs the International EMF Project that will result in major reviews of health effects of static, low-frequency and high frequency electromagnetic fields ([www.who.int/peh-emf](http://www.who.int/peh-emf)). The state of science that is, necessarily brief and sketchy, presented in this contribution is drawn from the reviews of the abovementioned organizations. No references are provided to individual studies. Instead, a (non-exhaustive) reference list is given with the main recent reviews and reports.

## Electromagnetic spectrum

Electromagnetic fields come in many different forms. The basic characteristic is the frequency (expressed in hertz, Hz), that is coupled to the wavelength. The higher the frequency, the higher the intrinsic energy content of the fields. Fields with wavelengths shorter than 100 nm possess sufficient energy to break chemical bonds and to cause ionizations. Such fields are therefore named ionizing radiation. All other fields, including ultraviolet radiation, visible light, infrared (heat) radiation and radiofrequency and low-frequency fields form the non-ionizing part of the electromagnetic spectrum (fig. 1).

## Direct and indirect effects

Direct effects are the result of an interaction between the electromagnetic field and biological tissue. They may lead to biological or health effects (see below). Indirect health effect may occur when there is an interaction between electromagnetic fields and medical devices that contain electronics. Under certain circumstances external electromagnetic fields may interfere with electronic circuits of exposed equipment. This may lead to situations where these devices malfunction and the health of

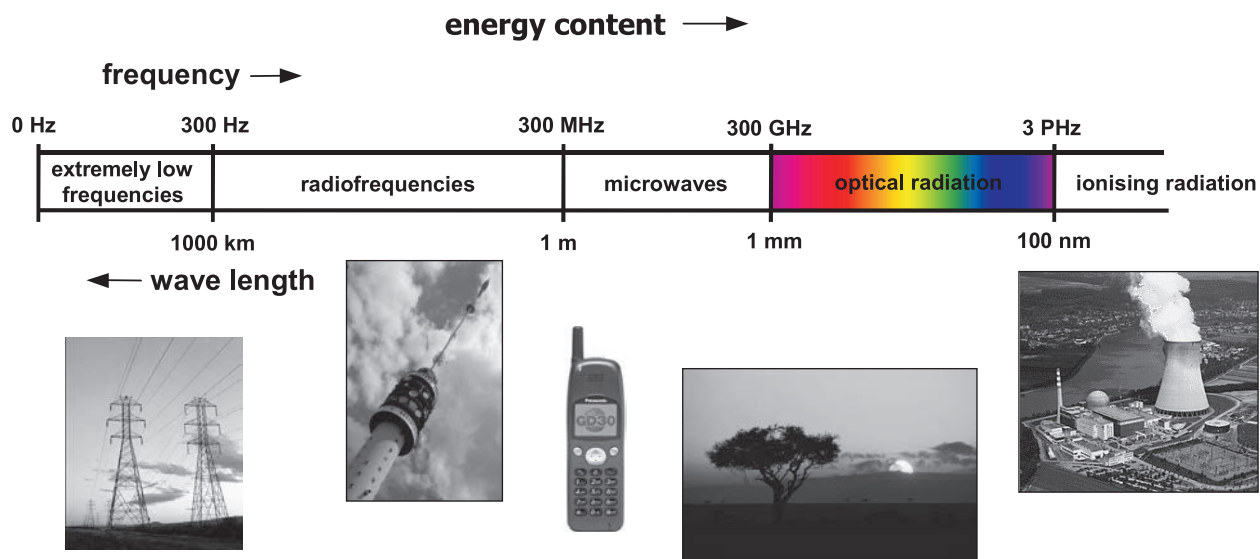


Figure 1. The electromagnetic spectrum.

people using them may be afflicted. Such devices include small and sometimes implanted devices such as cardiac pacemakers, insulin pumps and blood glucose meters, but also larger ones like electric wheelchairs. Indirect effects are the result of problems of a technical nature and are not further dealt with here. This contribution only discusses direct effects.

### Thermal and non-thermal effects

A distinction that is often made with regard to exposure to higher frequency electromagnetic fields is that between thermal and non-thermal effects. Thermal effects result from the fact that electromagnetic fields with frequencies above approximately 100 kHz may be partly absorbed by materials containing water (such as biological tissues) and be converted into heat. Excessive heating may lead to biological or health effects, as will be discussed below. Exposures in everyday life generally do not involve tissue heating, however, and therefore will not lead to thermal effects. Nevertheless, people fear that such exposures might still result in health effects, e.g. non-specific symptoms such as headache and sleeplessness or even life threatening effects like the induction of cancer. Because heating is not likely to occur, such effects are called non-thermal.

Sometimes accusations are made that non-thermal effects are not being considered in the analysis of the scientific information, because they are not used as a basis for exposure guidelines. This is not the case, however. The organizations mentioned above review all relevant studies, including those

looking at non-thermal effects. In several studies non-thermal biological effects have been demonstrated, but adverse health effects on the basis of such effects have not been established. Therefore they cannot serve as a basis for exposure guidelines. It should be noted, however, that this only pertains to high frequency fields. Effects of low-frequency fields are by nature always non-thermal.

### Short-term and long-term effects

Depending on when effects can be measured or observed, they are considered short or long-term effects. Short-term effects occur during or shortly after exposure. Long-term effects may not become manifest until months or years later. Of course every long-term effect is always the result of a short-term effect. At some point in time there should have been an interaction between the electromagnetic fields and biological tissue.

### Biological and health effects

In the interpretation of the data on the effects of non-ionizing radiation it is important that a distinction is made between biological effects and (adverse) health effects. A biological effect is any influence of a chemical, physical or biological factor on the resting state of a biological system. That can be a cell, a tissue, an organ or an entire organism. Only when the natural compensatory mechanisms can no longer adequately deal with the external influence and the system is affected outside of its natural bandwidth, an adverse health effect may result. So when in, for instance, *in vitro* studies an effect on certain cell types is demonstrated, this does not necessarily mean that this

same effect will result in an adverse health effect in an organism. Even when a certain factor is demonstrated to affect experimental animals, the same effect does not necessarily also occurs in humans. It should be noted, however, that effects demonstrated in experimental animals are much stronger indications for possible effects in humans than effects found in vitro. In summary: a biological effect is not the same as, or does not necessarily result in, an adverse health effect.

## Static fields

### Short-term effects

Static electric fields induce a surface charge on the body. This can lead to the movement of hairs and perception of the field. The threshold for this effect is a field strength of approximately 20 kV/m. If a charged person that is insulated touches a grounded object, a small spark discharge may occur. This happens, for example, when walking over a synthetic carpet in a dry environment. Depending on the conditions, the field strength generated in this situation can range from around 10 kV/m to more than 1200 kV/m. These discharges do not result in adverse health effects. They may, however, cause discomfort and startle responses. Annoyance may occur above 25 kV/m.

Static magnetic fields can interact with organisms by different mechanisms. By a process of magnetic induction, charged particles moving in a static field can give rise to electric fields and currents. This can result in the generation of small electric currents in the blood. Induction of this kind also occurs when an organism moves through a static field. According to Faraday's Law, small electric currents will then be generated in the body.

Magnetomechanical effects are a second mechanism. These can result in molecules and larger structures being oriented in a static field (similar to the working of a compass). The biological effects of this type of interaction are (at least in human beings) negligible, since the number of natural magnetic substances present in the body is extremely low.

The third type of effect relates to interactions between molecules. A static magnetic field can exert an influence on certain intermediate products of chemical reactions whereby the rate of those reactions can change. For reactions involving the formation of radicals as intermediate products, it has been suggested that an influence would be

detectable even at field strengths of 10 mT. However, biological effects have never been discovered at such low field strengths.

Biological effects have not been unequivocally demonstrated at field strengths below about 2 T. In humans, movement of the head in a strong magnetic field sometimes invokes effects such as vertigo, nausea, headache, metallic taste and phosphenes. At field strengths below 2 T, such effects have not been observed.

### Long-term effects

There is no information on possible effects of chronic exposure, but long-term exposure to high field strengths in practice does not occur. The strength of the natural magnetic field varies between approximately 35 µT at the equator and 70 µT on the geomagnetic poles.

## Low-frequency fields

### Short-term effects

The physical effects of exposure to alternating fields with frequencies up to several MHz is the induction of electric fields and currents in tissues. These can result in biological and adverse health effects and provide the basis for exposure limits. The principal biological effect is stimulation of electrically excitable tissues such as the nervous systems.

The most serious effects, which can be life-threatening, are cardiac arrhythmias. At 60 Hz - i.e. within the range in which sensitivity is greatest - the minimum current density that is required for ventricular fibrillation (the uncontrolled contraction of the muscle fibres of the ventricle, resulting in drastic reduction of the heart's pumping action) is around 2.5 A/m<sup>2</sup> in experimental animals. It can be regarded as a conservative limit value for stimulation of the heart in human beings. The current density values which result in excitation of the heart lie at around 40% of the levels that cause fibrillation, consequently at approximately 1 A/m<sup>2</sup>. This value, which can be regarded as the estimated value of a 'lowest observed adverse effect level', corresponds closely to that of the minimum current density required for stimulation of nerve fibres: 1.2 A/m<sup>2</sup>.

The most significant effect at lower current densities is the occurrence of phosphenes. These are spots or flashes of light which are perceived in response to direct stimulation of the retina by elec-

trical current. They can, for example, result from an external electric or magnetic field. They generally disappear within an hour after exposure stops. A value of  $10 \text{ mA/m}^2$  can be regarded as a reasonable lower limit for the occurrence of phosphenes, observed at about 20 Hz. With both increasing and decreasing frequency, the current density required for the perception of phosphenes increases rapidly, and therefore the frequency range within which this phenomenon actually plays a role is limited from a few Hz to around 200 Hz.

### Long-term effects

The discussion on potential harmful effects of powerline frequency (50/60 Hz) fields has resulted from several epidemiological studies performed in the 1980's in the USA. These studies seemed to indicate an association between living near overhead powerlines (which was presumed to be associated with increased exposure to extremely low-frequency fields) and an increase in childhood leukaemia. This triggered a series of similar epidemiological studies in a number of countries throughout the world, as well as many laboratory studies into a possible mechanism that might explain the observed association. Also a number of diseases other than childhood leukaemia was studied.

The design and results of the epidemiological studies have been mixed. In general, assessment of exposure is a main problem, especially since it is not known what aspect of exposure (if any) is important. Most studies have been case-control studies, in which exposure is assessed sometimes many years after the critical period in the development of the disease. Nevertheless, several researchers have performed a pooled analysis of the raw data of what they considered to be the best available studies. These analyses came to the similar conclusion that there is a consistent statistical relationship between exposure to extremely low-frequency powerline magnetic fields higher than approximately  $0.4 \mu\text{T}$  and a doubling of the risk of childhood leukaemia. The question is, whether this conclusion can be generalized to all countries. Also, although a doubling of the childhood leukaemia risk seems serious, the impact of the presumed association is limited. For instance, it has been calculated that in the Netherlands one extra case of childhood

leukaemia in two or three years could result from magnetic field exposure, with an annual incidence of approximately 110 cases.

In 2002 the IARC, the International Agency for Research on Cancer of the WHO, performed a formal assessment of the carcinogenicity of static and extremely low-frequency electromagnetic fields. The IARC classified extremely low-frequency magnetic fields as "possibly carcinogenic to humans". Static electric and magnetic fields as well as extremely low-frequency electric fields were considered "not classifiable as to their carcinogenicity in humans". The classification "possibly carcinogenic" is based on limited evidence in humans, the childhood leukaemia data. For all other cancers in both children and human the evidence was considered inadequate. This was also the case for carcinogenicity in experimental animals.

What are the ramifications of these conclusions? It should be emphasised that this does not mean that extremely low-frequency magnetic fields are actually carcinogenic, simply that they might be. There is no evidence to support the existence of a causal relationship, nor has research yet uncovered any evidence that a causal relationship might exist. The IARC has classified more than two hundred agents as "possibly carcinogenic". However, not for all of these agents has their possible carcinogenicity lead to measures by the authorities to limit exposure. In many cases these are agents with which there is regular contact in daily life<sup>1</sup>.

### Radiofrequency fields

#### Short-term effects

The only scientifically established effect associated with exposure to radiofrequency (RF) electromagnetic fields is heating of tissues. An excessive rise in body temperature may result in adverse health effects, such as dehydration, heat shock and cardiovascular problems. The absorption of RF energy is expressed in the SAR, the Specific Absorption Rate. The SAR is a measure of the rate of uptake of electromagnetic energy in the body. With that it is a measure of the conversion of this energy into heat and therefore of heating. It is expressed in watts per kg bodyweight (W/kg). In animal experiments,

1 Examples of such agents include coffee, acetaldehyde (a substance naturally occurring in grapes and wine, and in higher concentrations in oxidised wines such as sherry and Madeira), pickled vegetables but also crude diesel oil, bitumen and carbon black (produced by burning scented candles and released into the air from toner during photocopying).

(behavioural) effects were observed with exposures resulting in an SAR of approximately 4 W/kg and higher. Experimental studies on humans indicated that healthy adult human beings can tolerate much higher exposures, but since the population also contains groups, e.g. young children, elderly people and diseased people, that might have less efficient thermoregulatory capabilities, it is generally accepted that exposure should not exceed 4 W/kg. In fact, many exposure limits and guidelines apply a large margin of safety resulting in a maximum permissible SAR of 0.08 W/kg for the general population.

With the increasing number of applications that result in low-level, often continuous exposure, increasingly questions are asked about possible non-thermal effects. For instance, the use of a cellular telephone results in exposure of part of the head, including brain tissue, that is not associated with any significant increase in temperature (maximally approximately 0.2 °C). Exposure of people living in the vicinity of base station antennas is much lower, albeit continuous, and is highly unlikely to be associated with any temperature increase. Still some people complain about non-specific symptoms such as headache, concentration problems, etc.

A increasing number of studies is being performed on a variety of endpoints. Several studies have measures cognitive functions during exposure to mostly handset-strength GSM-like signals. No consistent and reproducible effects have been found. In other studies, the influence of exposure to electromagnetic fields similar to those generated by a cellular phone on the natural electric activity in the brain during sleep has been studied. Characteristic brain wave patterns can be measured by making electroencephalograms. GSM-field exposure was shown to slightly modify some of these brain waves. Again, however, the effects were found to be not very consistent over the different studies. Moreover, any influence found did not seem to affect the way the test subject felt rested after the experiment - they even fell asleep somewhat earlier in some experiments - and it also had no influence on their health in general.

Several studies attempted in an experimental setting to invoke non-specific symptoms in people who complained about such symptoms and attributed them to electromagnetic field exposure. In none of these studies a relationship between exposure and symptom occurrence could be established.

In some biological systems effects have been found in laboratory experiments. Some years ago a study in which animals were exposed to cellular phone-like fields found DNA damage in brain tissue. Replication studies could not reproduce this effect, however. Recently, low level GSM-like fields were shown to result in DNA damage in cultured human cells. These data have not been confirmed thus far. Also membrane effects have been found in vitro, resulting in altered transmembrane transport of calcium, which might affect cellular functioning. It is not possible, however, to conclude that these effects will lead to adverse health effects. Such relationship has not been found and indeed it is very likely that there are many homeostatic mechanisms in an organism that compensate or annihilate effects of external factors.

In conclusion, thermal effects have been firmly established, but there is no or no clear and consistent evidence for health effects of a non-thermal nature. On the other hand, there is also no evidence for the absence of health effects. There are still a lot of questions, therefore further research should be performed.

### **Long-term effects**

The questions concerning possible long-term effects of RF electromagnetic field exposure mainly focus on cancer. A number of epidemiological and animal experimental studies has been published. One of the main problems in the epidemiological studies is exposure assessment. In most studies exposure has not been measured, but a proxy has been used, e.g. the distance of living to the source. In several countries, studies have been performed on people living near radio and television transmitters. Altogether, the results do not indicate that this is a risk factor for the development of cancer. In several other studies, occupational exposure has been estimated on the basis of job descriptions, also a very crude measure. No consistent association with the incidence of cancer emerges from that data.

In recent years, many studies have been done, or are still ongoing, on the effect of mobile phone use on the incidence of brain cancer. In several large cohort studies no associations were found with tumour incidence or mortality. The authors of some case-control studies, on the other hand, claimed to have found an association, but these studies had methodological shortcomings. The

general conclusion is, that clear, consistent evidence for an association between mobile phone use and cancer incidence is lacking. In the near future, the results from a large coordinated study in thirteen countries, the Interphone study, will provide valuable additional information.

In cancer bioassays - long-term exposure experiments in animals - no effect of such exposure at thermal or non-thermal levels has been observed. Also, no effect was found on growth and development of chemically-induced tumours. In one study, a stimulating effect was observed on the development of lymphomas in transgenic mice. A replication study found no effects, however, and also in non-transgenic mice no effect was observed on lymphoma growth or development.

Again, also for long-term effects no clear and consistent evidence for effects has been found. Although the animal studies do not provide indications for effects of long-term exposure, further epidemiological studies appear to be necessary. The presently available epidemiological data only pertains to relatively short exposure periods (measured on the human lifetime). The Interphone study will provide information on a longer exposure period, but further follow-up remains indicated.

## References

### Low frequencies

International Commission on Non-ionizing Radiation Protection (ICNIRP). Guidelines on limits of exposure to static magnetic fields. *Health Phys*, 1994; 66: 100-106.

International Commission on Non-ionizing Radiation Protection (ICNIRP). Guidelines on limits of exposure to time-varying electric, magnetic and electromagnetic fields (1 Hz - 300 GHz). *Health Phys*, 1998; 74: 494-522.

R. Matthes, A.F. McKinlay, J.H. Bernhardt, P. Vecchia, B. Veyret (eds.). Exposure to static and low frequency electromagnetic fields, biological effects and health consequences (0-100 kHz). Oberschleißheim: ICNIRP, 2003; publication nr ICNIRP 13/2003.

Health Council of the Netherlands: ELF Electromagnetic Fields Committee. Exposure to electromagnetic fields (0 Hz - 10 MHz). The Hague:

Health Council of the Netherlands, 2000; publication nr 2000/6E.

Health Council of the Netherlands: Electromagnetic Fields Committee. Electromagnetic Fields: Annual Update 2001. The Hague: Health Council of the Netherlands, 2001; publication nr 2001/14.

Health Council of the Netherlands: Electromagnetic Fields Committee. Electromagnetic Fields: Annual Update 2003. The Hague: Health Council of the Netherlands, 2004; publication nr 2004/01.

National Radiological Protection Board. ELF electromagnetic fields and the risk of cancer. Chilton, Didcot, Oxon: National Radiological Protection Board, 2001. Documents of the NRPB, Vol 12, No 1.

Assessment of health effects from exposure to power-line frequency electric and magnetic fields. NIEHS Working Group report. Research Triangle Park, NC: National Institute of Environmental Health Sciences, National Institutes of Health, 1998; publication NIH 98-398.

IARC Working Group on the Evaluation of Carcinogenic Risks to Humans. Non-ionizing radiation, Part 1: static and extremely low-frequency (ELF) electric and magnetic fields. IARC Monogr Eval Carcinog Risks Hum, 2002; 80: 1-395.

IEEE Standards Coordinating Committee 28. IEEE standard for safety levels with respect to human exposure to electromagnetic fields, 0-3 kHz. New York: The Institute of Electrical and Electronics Engineers, Inc., 2002; publication nr IEEE C95.6-2002.

Reilly JP. Applied bioelectricity. From electrical stimulation to electropathology. New York: Springer, 1998.

### High frequencies

International Commission on Non-ionizing Radiation Protection (ICNIRP). Guidelines on limits of exposure to time-varying electric, magnetic and electromagnetic fields (1 Hz - 300 GHz). *Health Phys*, 1998; 74: 494-522.

Independent Expert Group on Mobile Phones. Mobile phones and health. Chilton: Independent Expert Group on Mobile Phones, 2000.

National Radiological Protection Board: Independent Advisory Group on Non-ionising Radiation. Health effects from radiofrequency electromagnetic fields. Chilton, Didcot, Oxon: National Radiological Protection Board, 2003. Documents of the NRPB, Vol 14, No 2.

Health Council of the Netherlands: Radiofrequency Electromagnetic Fields Committee. Radiofrequency electromagnetic fields (300 Hz - 300 GHz). Rijswijk: Health Council of the Netherlands, 1997; publication nr 1997/01.

Health Council of the Netherlands: Electromagnetic Fields Committee. GSM base stations. The Hague: Health Council of the Netherlands, 2000; publication nr 2000/16E.

Health Council of the Netherlands: Electromagnetic Fields Committee. Mobile telephones. A health-based analysis. The Hague: Health Council of the Netherlands, 2002; publication nr 2002/01E

Health Council of the Netherlands: Electromagnetic Fields Committee. Electromagnetic Fields: Annual Update 2001. The Hague: Health Council of the Netherlands, 2001; publication nr 2001/14.

Health Council of the Netherlands: Electromagnetic Fields Committee. Electromagnetic Fields: Annual Update 2003. The Hague: Health Council of the Netherlands, 2004; publication nr 2004/01.

IEEE standards board. IEEE standard for safety levels with respect to human exposure to radio frequency electromagnetic fields, 3 kHz to 300 GHz. New York: The Institute of Electrical and Electronics Engineers, Inc., 1992; publication nr IEEE C95.1-1991.

Reviews of the effects of RF fields on various aspects of human health, commissioned by the IEEE ICES (International Committee on Electromagnetic Safety) Subcommittee 4 on RF standards. Bioelectromagnetics 2003; supplement 6, S1-S213.



# Blootstelling aan elektromagnetische straling tijdens MRI scanning

J. M. L. Engels  
Philips Medical Systems

## Samenvatting

MRI scanners zijn niet meer weg te denken uit de moderne ziekenhuizen en hebben hun beeldgevende en diagnostische waarde ruimschoots bewezen. Mede dankzij het feit dat bij MRI scanning er geen sprake is van ioniserende straling, kan een MRI opname veelvuldig herhaald worden en worden er ook vaak opnames van vrijwilligers gemaakt om weer nieuwe technieken en scanmethodes uit te proberen.

Zijn er echter niet toch ook mogelijke negatieve gezondheidseffecten verbonden aan het ondergaan van een MRI scan? De verschillende types van elektromagnetische velden die tijdens een MRI opname worden toegepast zullen worden beschreven en toegelicht, waarbij vooral gelet zal worden op de mogelijke negatieve gezondheidsaspecten, effecten van deze velden en de internationale regelgeving die dit moet voorkomen.

Concluderend mag gesteld worden dat er wel degelijke negatieve gezondheidsaspecten zijn waar rekening mee gehouden moet worden. De moderne MRI scanners zijn echter zodanig ontwikkeld en beperkt in hun mogelijkheden dat er voor de patiënt in ieder geval tot op heden geen blijvende negatieve gezondheidsaspecten zijn waargenomen en ook zijn er geen argumenten bekend waarom deze situatie in de naaste toekomst zou kunnen veranderen.

## Introductie

Recentelijk heeft Philips Medical Systems het 25 jarig jubileum gevierd van het succesvol verkrijgen van een eerste succesvol klinisch plaatje van een MRI scanner. De opname was gemaakt op het eerste proefmodel van een scanner destijds nog werkend bij een magnetische veldsterkte van slechts 0.15T (Tesla) en welke was geïnstalleerd in het laboratorium in Best. Het heeft vervolgens nog 4 jaren geduurd voor de eerste klinische scanner geïnstalleerd kon worden in een ziekenhuis. De sterke van het magneetveld was inmiddels opge-

voerd tot 0.5 T en de magneet was een supergeleidende magneet (in tegenstelling tot de eerste elektromagneet die nog gewikkeld was van koperdraad en bij kamertemperatuur werkte).

Sinds die tijd is er enorme vooruitgang geboekt. Wereldwijd wordt er geschat dat er nu al zo'n 25.000 scanners zijn geïnstalleerd en dat er meer dan 500 miljoen patiënten zijn gescand. Naast Philips zijn het vooral Siemens en General Electric die de meeste scanners geproduceerd en operationeel hebben. Tegenwoordig heeft ieder ziekenhuis toch wel minstens één MRI scanner tot zijn beschikking. De grotere ziekenhuizen hebben er vaak al meerdere in gebruik. In enkele academische ziekenhuizen wordt zelfs al gewerkt met MRI scanners met een magneetveld van 7.0 T, waar vooral nog research gericht onderzoek mee gedaan wordt en zelfs zijn er al enkele scanners die werken bij 9.4 T. MRI scanners hebben zo snel hun toepassing in het ziekenhuis kunnen vinden omdat niet alleen de resulterende opnames meestal voor zich zelf spreken (de anatomie is overduidelijk zichtbaar en de diagnose relatief gemakkelijk te maken) wat betreft de beeldkwaliteit, maar vooral ook omdat het aantal toepassingen en variatie mogelijkheden enorm is en daardoor MRI niet alleen geschikt maakt voor opnames van 'zacht weefsel', maar nog vele andere toepassing al bekend zijn en nog meer toepassing in het verschiet liggen. MRI opnames zijn 3 dimensionale opnames waarbij scannen in alle richtingen mogelijk is zonder dat de patiënt zich hoeft te verplaatsen. Het oplossend vermogen is zo goed dat gemakkelijk opnames met submillimeter resoluties gemaakt kunnen worden, waarbij diagnostische afbeeldingen gemaakt worden van anatomieën maar ook video's van bewegende lichaamsdelen (het hart of de ledematen) en zelfs functionele afbeeldingen gemaakt kunnen worden (hersenactiviteiten, diffusie van vloeistoffen).

## MRI principes

Bij het maken van een MRI opname wordt er specifiek gebruik gemaakt van de magnetische eigenschappen van de protonen. Omdat deze eigenschappen afhankelijk zijn van het soort weefsel (type orgaan, ...) en de conditie van dit weefsel (goedaardige of slechtaardige tumoren, ...) waarin de protonen zich bevinden, zijn MRI opnames bijzonder geschikt om zeer duidelijke opnames te maken van de anatomie van de mens. De magneetvelden van deze MRI scanners, nodig om de protonen het gewenste magnetische moment te geven, variëren van 0.2 T tot 3.0 T, waarbij verreweg het grootste aantal 1.5 T als magneetveld heeft. Hoe hoger de magneetveld sterkte des te meer signaal kan er verkregen worden en dus zullen de resulterende afbeeldingen van hogere kwaliteit zijn. De meeste systemen zijn als cylindrische magneten uitgevoerd, zie Fig 1.

Naast de alsmaar sterker wordende statische magneetvelden, worden de toegepaste geschakelde magneet gradiëntvelden, die nodig zijn voor de lokalisatie van het signaal afkomstig van de protonen, ook alsmaar sterker, dat wil zeggen ze hebben een grotere magneetveldsterkte en kunnen sneller aan- en uitgeschakeld worden. Het resultaat is dat de veranderingen in de gradiënt magneetveldsterkte uitgedrukt in Tesla per seconde steeds

groter worden en in de orde van grootte van 10 tot 100 T/s kan bedragen.

Het uiteindelijke MRI signaal dat gebruikt wordt om de afbeeldingen te construeren wordt verkregen met behulp van de RF antenna's, of te wel de RF spoelen. De RF spoelen worden als zend- en ontvangstspoelen gebruikt, maar ook is het mogelijk om naast de zendspoel nog aparte, op de anatomie geoptimaliseerde, ontvangst RF spoelen te gebruiken, zie Fig. 2.

Met de zend RF spoel worden de protonen kortstondig geëxciteerd, daarna wordt het signaal van de relaxerende protonen ontvangen met de ontvangst RF spoel en wordt de data gereconstrueerd en als beeldopname gepresenteerd aan de gebruiker. Ook de gebruikte hoeveelheid RF energie tijdens de MRI scan, waarmee de protonen worden geëxciteerd, is gemaximaliseerd en moderne scanners gebruiken steeds vaker het maximaal toegestane niveau voor de RF energie.

## EM Velden gegenereerd tijdens een MRI scan

Drie basis componenten van het MRI systeem, de magneet, de gradiënt magneten en de RF zend spoelen genereren specifieke elektromagnetische velden tijdens het scannen.

Het sterke statische magneetveld genereert een veld met uiteraard een frequentie van 0 Hz. In het centrum van de magneet is dit magneetveld homogeen hetgeen essentieel is voor de MRI scanning techniek. Direct buiten de scanner is er natuurlijk sprake van het strooiveld hetgeen niet verwaarloosbaar klein maar zelfs nog zo sterk is dat in de praktijk dit strooiveld de grootste gevaren oplevert voor de gezondheid. Vele ongelukken zijn al

Figuur 1



Figuur 2



gerapporteerd waarbij kleine maar ook grote magnetische objecten als projectielen de magneet invlogen en soms dus patiënten hebben verwond. De geschakelde gradiënt magneetvelden kunnen diverse golfvormen hebben, zowel sinusvormige als trapezoïde golfvormen worden toegepast, waarbij de stijgtijden van de magneetvelden in de orde van grote van een milliseconde zijn en dus de gegeneerde elektromagnetische velden in het frequentie gebied rond de kHz liggen.

De RF energie van de RF zend spoelen hangt direct samen met de sterkte van het statische magneetveld en wordt bepaald door de Larmor frequentie van de protonen bij dit magneetveld. Deze frequentie is 42 MHz per Tesla.

De drie soorten elektromagnetisch velden waar tijdens een MRI opname de patiënt en soms ook het personeel aan worden blootgesteld zijn dus velden in de frequentie gebieden van 0 Hz, rondom de kHz en enkele tientallen MHz'en.

### Toegestane limietwaardes

Voor de veiligheid van medische systemen bestaan een aantal internationaal erkende standaards, gepubliceerd door de IEC (International Electrotechnical Commission). Specifiek voor MRI scanners betreft dit de IEC60601-2-33, 2nd edition, 2002, waarin alle begrenzingen voor de sterkte van de elektromagnetische velden staan beschreven, maar wel alleen specifiek voor de patiënt. De IEC heeft specifieke werkgroepen die verantwoordelijk zijn voor hun standaard. Deze werkgroepen worden samengesteld uit leden afkomstig uit de industrie, de overheid en wetenschappelijke experts en vormen als zodanig een goede mix van de verschillende belangengroepen. Er bestaan reeds vergevorderde plannen om de standaard uit te breiden met ook begrenzingen en beperkingen voor de blootstelling aan elektromagnetische velden voor het personeel dat met MRI scanners moet werken, zowel in het ziekenhuis als bij de MR fabrikant.

De oorsprong van de beschreven limietwaardes moet gevonden worden in de publicaties van de International Commission on Non-Ionizing Radiation Protection (ICNIRP), die algemene richtlijnen geven voor de beperking aan blootstelling van elektromagnetische velden in het frequentiegebied tussen 0 Hz and 300 GHz.. De ICNIRP formuleert zijn limietwaardes specifiek voor patiënten, personeel en voor het algemene publiek. De ICNIRP is samengesteld uit experts, echter experts werkzaam bij de industrie kunnen nooit lid worden van de ICNIRP! De ICNIRP moet dus een

enorm breed gebied van toepassingen afdekken en formuleert de richtlijnen in principe als input voor IEC (of andere) standaardisatie organisaties, die dus geacht worden de ICNIRP richtlijnen over te nemen in hun standaarden.

In de loop van de tijd heeft ICNIRP ook richtlijnen gepubliceerd specifiek voor de patiënten van MRI scanners, echter tegelijkertijd en soms eerder heeft de IEC werkgroep verantwoordelijk voor de IEC60601-2-33, haar standaard gepubliceerd. Hierdoor zijn er verschillen ontstaan in de richtlijnen die wellicht in de naaste toekomst voor praktische problemen kunnen gaan zorgen. Specifiek voor de patiënten limietwaardes zijn er nauwelijks of geen verschillen tussen ICNIRP en IEC, maar specifiek voor personeel werkend met de MR scanners kunnen deze verschillen wel ontstaan. Hierbij mag en moet aangetekend worden dat de ICNIRP alleen richtlijnen formuleert voor personeel in het algemeen en dus niet specifiek voor MR personeel en dus ook niet de specifieke sociale en economische aspecten van belang voor deze categorie personeel en de sociale consequenties in rekening kan brengen. Dit constaterende geeft een voldoende argument om de richtlijnen van ICNIRP voor MR personeel opnieuw te beschouwen en te heroverwegen.

### Gezondheidsaspecten

#### Het statische magneetveld

Er is bijzonder veel wetenschappelijk onderzoek gepubliceerd naar mogelijke gezondheidsaspecten die samenhangen met blootstelling aan statische magneetvelden. Voor MRI scanners moet er rekening worden gehouden met zowel de effecten voor de patiënt in het systeem tijdens de MRI scan, als naar effecten voor het personeel werkend rondom het systeem in het strooiveld van de magneet. Voor supergeleidende magneten moet er vooral beseft worden dat dit magneetveld altijd aanwezig is en dus niet alleen tijdens het scannen van de patiënten. Bovendien moet er rekening gehouden worden met instantane effecten en met mogelijke cumulatieve effecten.

Magneto hydrodynamische effecten worden pas verwacht bij zeer hoge magneetvelden ( $>10T$ ) en theoretische modellen zijn ontwikkeld om de krachten die ontstaan op stromend bloed (een diëlektrische vloeistof) te berekenen. Bij de magneetvelden toegepast bij routine MR scanners ( $<3T$ ) zijn deze krachten echter nog zeer klein en niet van

biologisch belang. Andere mechanismes voor de interactie tussen mensen en magneetvelden zijn niet goed bekend. Wel is algemeen bekend uit vele publicaties dat er een sensorisch effect optreedt als een persoon zich beweegt in een magneetveld  $>1.5\text{ T}$ . Dit effect kan aanleiding geven tot misselijkheid of duizeligheid. Ook worden effecten als metaalmaak en hoofdpijn genoemd. Deze effecten zijn echter zeer subjectief en kortstondig (zijn alleen aanwezig tijdens blootstelling aan het magneetveld). Ook is bekend dat deze effecten ernstiger worden naar mate het magneetveld hoger is. Niet geheel zeker is of de effecten het gevolg zijn van blootstelling aan het magneetveld of juist alleen ontstaan als de betreffende persoon zich beweegt in het magneetveld, waarbij het zelfs nog mogelijk is dat alleen beweging in het inhomogene strooiveld van de magneet de effecten veroorzaakt. Zeker is dat patiënten in systemen tot  $3\text{ T}$  nooit klagen over deze effecten waarbij er uiteraard geconstateerd moet worden dat patiënten tijdens de opname niet bewegen in het magneetveld. Er is tot op heden geen enkel bewijs voor enig cumulatief gezondheidsaspect gerelateerd aan blootstelling aan een statisch magneetveld

### **Het geschakelde gradiënt magneetveld**

Vanaf het moment dat de geschakelde gradiënt magneetvelden krachtiger werden (in de negentiger jaren) is bekend dat bij patiënten er sprake kan zijn perifere spier stimulaties. Omdat er verschillende golfvormen voor de geschakelde gradiënten gebruikt worden is niet eenduidig de relatie met het frequentiegebied te leggen. Geschat wordt dat we te maken hebben met het gebied rond de  $\text{kHz}$ . Ook zijn er publicaties van effecten in het centrale zenuw stelsel als gevolg van blootstelling aan geschakelde magneetvelden die aanleiding geven tot stimulaties van de oogzenuwen (lichtflitsen). Deze effecten spelen zich echter vooral bij iets lagere frequenties af. Bovendien zijn er geen publicaties die dit effect beschrijven gerelateerd aan de geschakelde gradient magneetvelden bij MRI. De door de IEC gehanteerde limietwaarden zijn gericht op voorkoming van pijnlijke perifere spier stimulaties. De grenswaarden worden uitgedrukt in Tesla per seconde, een grootheid die gemakkelijk gerelateerd kan worden aan de gradiënt velden die bij MRI gebruikt worden. De feitelijke grenswaarde is afhankelijk van de toegepaste MR scan methode, is in de orde van grote van  $50\text{ T/s}$ . Van belang is nog het feit dat deze grenswaarde voor voorkoming van perifere spier stimulaties onaf-

hankelijk is van de gebruikte magneetveldsterkte van het systeem.

Ook ICNIRP heeft voor de patiënten de perifere spier stimulaties als relevante fysiologisch proces geaccepteerd voor de MRI patiënten. Voor personeel hanteert ICNIRP echter de lagere limietwaarden die gekoppeld zijn aan de effecten in het centrale zenuwstelsel. In de praktijk kan dit een probleem opleveren aangezien de gradiëntvelden weliswaar alleen aanwezig zijn tijdens het scannen, maar de strooivelden van deze gradiënten zijn nog aanzienlijk vlak buiten de scanner waar eventueel personeel zich kan bevinden tijdens het scannen. Dit strooiveld kan hoger zijn dan de door de ICNIRP aangegeven limietwaarde. Voor personeel dat zich tijdens het scannen bij de scanner bevindt moet vooral gedacht worden aan doctoren die interventioneel met de patiënt een onderzoek uitvoeren en daartoe dus tijdens het scannen en gestuurd door real time of snelle opnames hun onderzoek uitvoeren. De relevante vraag is nu of ook voor het personeel de grenswaarden gerelateerd aan het voorkomen van perifere spier stimulaties niet geaccepteerd kan worden als grenswaarde.

### **Het RF veld**

Al vanaf de begin jaren van de toepassingen van MRI, is bekend dat met name de RF energie beperkt moet worden. Te veel RF energie in het MHz frequentiegebied zal resulteren in een te hoge temperatuurverhoging van het weefsel van de patiënt. Al in de tachtiger jaren is geaccepteerd dat voor patiënten een maximale temperatuur verhoging van  $1^\circ\text{C}$  acceptabel is en alleen voor bepaalde categorieën patiënten (bijvoorbeeld voor patiënten met een slechte bloedcirculatie) is dit nog verder beperkt tot een verhoging van maximaal slechts  $0.5^\circ\text{C}$ . Deze gemiddelde temperatuurverhoging voor de patiënt wordt beperkt door het RF vermogen gemiddeld over het totale gewicht van de patiënt te beperken. Dit vermogen wordt uitgedrukt in de grootheid SAR (Specific Absorption Rate). Voor een patiënt betekent dit in de praktijk dat de SAR minder moet zijn dan  $4\text{ W/kg}$  gemiddeld gemeten over een periode van 6 minuten. Omdat de RF energie niet altijd over het gehele lichaam (whole body SAR) gelijkelijk wordt verdeeld kan de SAR ook worden uitgedrukt in een 'hoofd SAR' of in de 'lokale SAR' (gemeten over iedere willekeurige 10 gram weefsel van de patiënt).

In de begin jaren van MRI was de SAR nog geen belangrijke beperking voor de toegepaste MRI technieken. Met de moderne scanners, zeker bij de hogere magneetvelden, wordt echter veel vaker de maximale toegestane hoeveelheid SAR toegepast. In de praktijk kan dit aanleiding geven tot een warmte sensatie voor de patiënt en uiteindelijk kan dit zelfs aanleiding geven tot een verhoogde transpiratie van de patiënt.

Door de IEC en de ICNIRP worden vergelijkbare waardes gehanteerd voor de toegestane SAR voor patiënten. ICNIRP heeft een extra veiligheidsfactor 10 ingevoerd voor personeel in het algemeen en dus ook voor MRI personeel. Omdat de RF zend spoel een zeer beperkt strooiveld heeft, zal in de praktijk de blootstelling aan RF energie tijdens het scannen nog zeer gering zijn en dus, hoewel de factor 10 wel erg conservatief is (in de praktijk een gemiddelde temperatuurverhoging van slechts 0.1°C zal geven), zal dit geen praktische problemen geven in de klinische praktijk.

Van belang is nog om te realiseren dat de SAR limietwaardes onafhankelijk zijn van het toegepaste statische magneetveld. In de praktijk is het wel zo dat bij MRI systemen met een hoger statisch magneetveld het gebruik van de maximaal toegestane SAR vaker voorkomt in de klinische praktijk, omdat er bij hogere magneetvelden meer energie nodig is om de protonen te exciteren. Ook is de interactie tussen de RF straling en het weefsel van een andere aard bij systemen met een hoger magneetveld als gevolg van het feit dat de frequentie van de RF energie hoger is (recht evenredig met de magneetveldsterkte toeneemt). Recent uitgevoerde simulaties voor de RF interactie met modellen van de menselijke anatomie, geven aan dat vooral de lokale SAR van groter belang wordt en dat dus niet altijd de whole body SAR de limiterende factor zal zijn. Praktische vraagstelling is dan echter hoe een patiënt het lokale SAR effect (en de daarmee gepaard gaande lokale onderhuidse opwarming zal waarnemen.

## Internationale standaarden

Uit het voorgaande is al duidelijk geworden dat er voldoende internationale regelgeving is om de veiligheid van een MRI scan te garanderen voor patiënten. Pas de afgelopen jaren is er discussie ontstaan over de veiligheid van het personeel dat werkt met de MRI scanners. Dit personeel bestaat dus uit de operators en medische doktoren in het ziekenhuis, maar ook uit het personeel bij de MR

fabrikanten, zoals de ontwikkelaars, technici in de fabricage omgeving en ook de service engineers die het systeem moeten onderhouden nadat het geïnstalleerd is in het ziekenhuis. Met name voor het personeel was nog geen regelgeving voor handen hoewel er door de ICNIRP wel limietwaardes geformuleerd zijn. Deze voorgestelde limietwaardes zijn nu recentelijk (in april 2004) in Europa overgenomen in een nieuwe Europese wetgeving, echter zonder rekening te houden met het speciale sociale karakter van het soort personeel dat met MRI scanners werkt. Hierdoor dreigt een situatie te ontstaan waardoor de toepassingen van MRI voor patiënten beperkt kunnen worden, vanwege algemene beschermende bepalingen voor het personeel. Als echter de sociale relevante en het feitelijke risico voor het personeel worden afgewogen mag worden verwacht dat de Europese regelgeving genuanceerder toegepast mag worden. De verantwoordelijke IEC werkgroep heeft recentelijk een nieuwe werkopdracht geaccepteerd om ook de internationale regelgeving voor de blootstelling van MRI personeel aan de elektromagnetische straling geproduceerd door een MRI scanner in de bestaande IEC 60601-2-33 standaard op te nemen. Dit zal mogelijk resulteren in een amendement op de huidige standaard dat als het door de landen die de IEC standaarden erkennen hopelijk nog in 2007 geaccepteerd zal worden.

## Conclusies

Ook voor MRI scanners zijn er beperkingen geformuleerd in internationale standaarden om de veiligheid van de patiënten en het personeel te garanderen. De in deze standaarden gekozen limietwaardes voor de elektromagnetische straling die gebruikt wordt tijdens het scannen met een MRI scanner, zijn zodanig geformuleerd dat er geen kortstondige of blijvende gezondheidseffecten verwacht worden. MRI scans kunnen tot op heden zo vaak worden herhaald als maar wenselijk is voor het onderzoek van de patiënt. Toch zijn er wel degelijk gezondheidsaspecten waar bij het ontwerpen van MRI scanners rekening mee moet worden gehouden. Deze effecten, te weten dus de kortstondige effecten van het bewegen in het statische magneetveld, de mogelijk perifere spierstimulaties van de geschakelde gradiënt magneetvelden en de minimale opwarming als gevolg van de RF energie, zijn echter instantaan en zijn tot op heden geen aanleiding geweest tot rapportage en meldingen van nadelige langere termijn effecten die gerelateerd kunnen worden aan MRI opnames.

MRI opnames kunnen dus nog steeds gezien worden als veilig voor de patiënt, hoewel er natuurlijk toch ook rekening gehouden moet worden met diverse mogelijke situaties tijdens een MRI opname die letsel aan de patiënt kunnen toebrengen. Het grootste gevaar bij een MRI opname is het rondom de magneet altijd aanwezige magnetenveld. Er zijn meerdere ernstige ongelukken gerapporteerd waarbij zware magnetische voorwerpen als projectielen de magneet invlogen en letsel hebben toegebracht aan de patiënt. De voorzorgsmaatregelen in het ziekenhuis moeten dan ook streng in acht genomen worden. Ook zijn er contra-indicaties voor patiënten die in acht moeten worden genomen. Patiënten met implantaten mogen namelijk niet gescand worden vanwege de

mogelijke interactie tussen dit implantaat en de elektromagnetische velden die toegepast worden tijdens de MRI scan. Deze interactie kan het functioneren van het implantaat negatief beïnvloeden (bijv. een pacemaker) of kan tot ongewenste opwarming van het implantaat aanleiding geven. Ook is het mogelijk dat de toegepaste RF energie aanleiding geeft tot lokale RF interactie met de patiënt of met accessoires gebruikt tijdens het scannen (bijv. ECG electrodes). Deze interactie kan weer aanleiding geven tot lokale verhitting die zelfs kan leiden tot zogenaamde RF brandwonden. Al deze effecten zijn uiteraard te voorkomen door zorgvuldig gebruik en toepassing van de instructies.



# Software Defined Radio in reconfigurable logic

H.J.W. Medenblik, R.M.E.M van Heijster  
TNO Defence, Security and Safety  
Henk.Medenblik@tno.nl  
Rob.vanHeijster@tno.nl

## Introduction

Software Defined Radio (SDR) is a rapidly evolving technology that allows easy adaptation to different communication standards without changing the actual hardware platform. To cope with ever increasing communication needs, analog radio systems are more and more being replaced by digital radio systems. The need for increased spectral efficiency led to the application of new modulation schemes that could only be implemented using digital technology. By implementing digital radio systems in reconfigurable hardware we get to the concept of Software Defined Radio. A system based on SDR can be used in a wide range of communication standards and hence applications.

Within this article the concept of SDR is outlined as well as the applicable hardware platform. SDR developments at TNO are shown, using the design flow as a guide line. Finally two examples of SDR based systems developed by TNO are given.

## Ideal versus practical SDR

The ideal Software Defined Radio concept is shown in Figure 1, where A-to-D and D-to-A converters are connected directly to the Digital Signal Processing block. Received signals are sampled without frequency conversion and processed into the digital domain. In opposite direction, the transmit

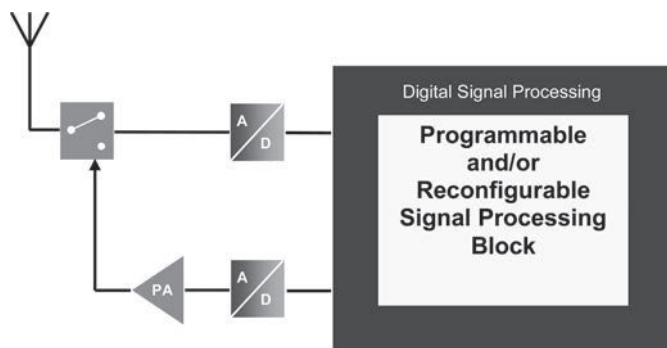
signal is constructed in the digital domain at the required transmit frequency. All processing is performed in the digital domain using the signal processing block and adaptation to any radio standard is possible by only reconfiguring the digital signal processing block.

In most cases the ideal SDR concept of Figure 1 is not feasible given current state of the art of digital signal processing hardware technology. Extremely fast and linear A-to-D and D-to-A converters and very fast signal processing logic are required. Even when feasible, form factor and cost aspects can prevent the usage of the ideal SDR concept. However, both feasibility and cost will benefit from the application of frequency conversion in the analog domain, as is shown in Figure 2, the feasible SDR concept. The received signal is converted to a lower intermediate frequency (IF), passed through a bandpass filter in order to remove wideband noise and possible aliases and to gain frequency selectivity before it is applied to the receiver A-to-D converter.

In reverse direction the transmit path consists of a signal processing block which performs modulation and conversion to an intermediate frequency. It will be converted to the analog domain and fed to an analog bandpass filter (e.g. SAW device, helical) in order to remove undesired spurious and aliasing products which result from imperfections in the signal processing domain. The transmit signal is up-converted to the final RF frequency, amplified and fed to the antenna.

The analog front-end design should not be underestimated in SDR. New standards put increasingly stringent requirements, especially with respect to phase noise and linearity. On the other hand, SDR

Figure 1: Ideal software defined radio concept.



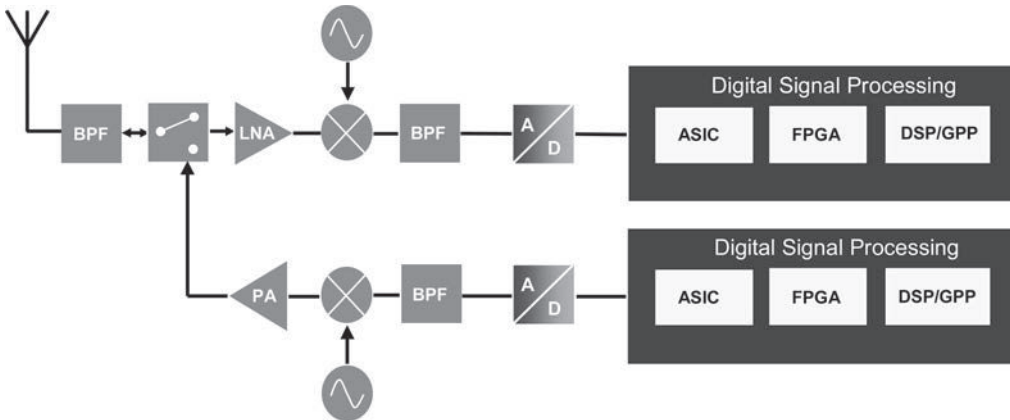


Figure 2: Feasible SDR concept with analog frontend

can help to meet these specifications in combination with dedicated front-end topologies.

### SDR Hardware

Focusing on the digital part of feasible SDR, the actual signal processing is often performed at baseband or at the lower IF. Various signal processing functions are required in software defined radio. Examples are digital up and /or downconversion, pulse shaping filters, FFT processing blocks, interpolators, decimators, adaptive equalizers, symbol mappers, symbol slicers and forward error correction. Dedicated hardware components are needed to accomplish all these signal processing functions. These components can be divided into four categories:

- ASICs.  
Application Specific Integrated Circuits (ASIC) are suitable for very generic and processing - intense SDR functions. An example of that is the digital downconverter (DDC) block.
- FPGAs  
Field Programmable Gate Arrays (FPGA) allow

us to perform high-speed (parallel) signal processing by means of a fully reconfigurable and flexible component.

- DSPs

Digital Signal Processors (DSP)) are very easily reprogrammable by means of a software change.

- GPPs

General Purpose Processors (GPP) consists of devices ranging from a simple microcontroller device up to fast Intel Pentium like processors. Although the faster type of GPPs can perform simple signal processing functions, in general the GPP is not specifically designed to perform fast signal processing functions. Therefore they are commonly used at the back-end of the system, where processing speed is of less importance and flexibility requirements are tight. An example is data encryption.

Table 1 shows a comparison between these various categories of signal processing components with respect to flexibility, cost, power consumption, computing power and program reusability.

Table 1: Comparison between different categories SDR HW components

	ASIC	FPGA	DSP	GPP
Flexibility	--	+	++	++
Costs	+/-*	-	+	+
Power Consumption	++	-	0	0
Computing power	++	+	0	-
Program reusability	0	+/0	+	++

\* ASICs price depends largely on quantity.

ASICs are the best choice when it comes to computing power. However they lack in flexibility and are only economically feasible in large quantities. On the other side, DSPs are very flexible but their computing power is much less compared to ASICs due to their serial processing nature. The GPP is generally not the best choice for fast signal processing. A good alternative for large signal processing power and flexibility is the FPGA which therefore seems to be a good choice for software defined radio hardware.

## Applications of SDR Technology

Some SDR developments at TNO are shown, using the design flow as a guide line. These examples underline the necessity of a sound design flow.

### Design flow

The design starts generally with the draw-up of a high level system model in one of the available system simulation tools (Matlab, SPW, SystemView, ADS). The high abstraction level of this system model allows simulation and analysis of the desired system performance and requirements of the transmit/receive path.

The next step in the design process is the conversion of the system model to a more detailed model that includes quantization in order to analyze the impact on overall system performance. In this stage of the design a balance is made in order to achieve system performance using minimal hardware resources. Several iterations might be required before this optimum is achieved. Various design tools can be used in combination to evaluate the system performance. As an example, the evalua-

tion of the performance of a digital modulator can be done with the Agilent Vector Signal Analyzer post processing software application while the system simulator in Matlab or SystemView is used for generation of the simulation data.

The third step is the conversion to a VHDL implementation model. In this stage the design is separated into smaller building blocks. The results from the VHDL simulations (Modelsim VHDL simulator) are compared with both the output of the high level system simulation and the output of the quantized system model.

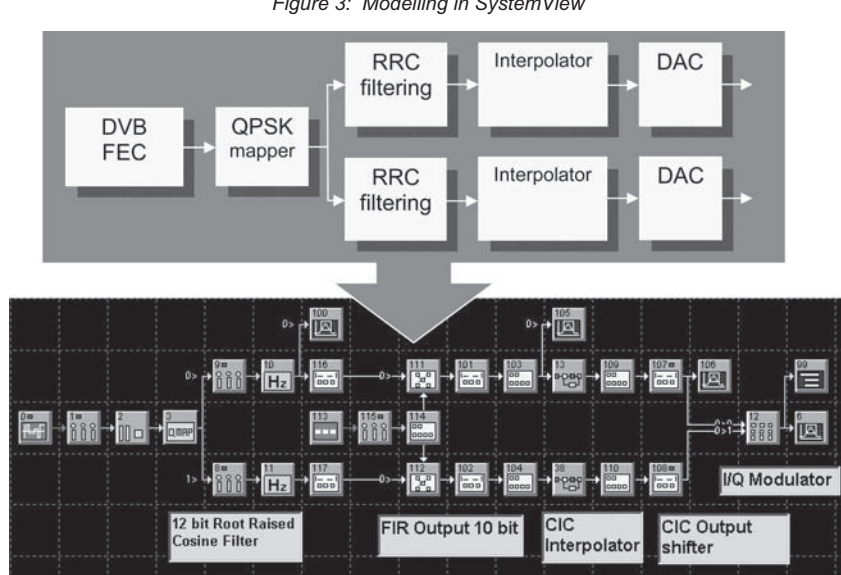
The last step is the mapping of the design in hardware by downloading a programming file into the FPGA. The test vectors are used to evaluate the hardware implementation and to compare the results with that of the various simulations performed.

### QPSK DVB Modulator

The first example of the described design flow is the design of a digital modulator for implementation in a FPGA.

The design objective aimed at a QPSK modulator according to DVB specifications that had to fit in a single small and cheap FPGA. The actual signal-processing block comprises the full signal path including forward error correcting blocks, symbol mapping, I and Q channel pulse shaping and a programmable interpolator. The output of the FPGA is fed to a dual channel transmit D-A converter running at a 100 MHz sample rate.

Figure 3: Modelling in SystemView



The system specification required a spurious and noise level below -55 dB at the adjacent channel and an Error Vector Magnitude (EVM) of 0.9 % maximum. EVM is a performance measure in digital communications indicating the phase and amplitude error between an ideal vector and actual measured vector (constellation point).

The design flow of the digital modulator started with the draw-up of a system model in SystemView, see Figure 3. This model was used to determine block requirements, the minimal impulse length of the symbol shaping FIR filters and the D-to-A converter requirements. This model was transformed in a second model that allowed analysis of quantization and truncation effects at several stages of the design and analysis of the resulting EVM and spectral efficiency. A trade-off was made between optimal oversampling ratio of the pulse shaping filters and the corresponding hardware size. Due to the limited FPGA resources a programmable Cascaded Integrator Comb interpolation filter was chosen for the programmable interpolator. Several iterations have been per-

formed before an optimum was achieved between performance and final hardware size.

The expected performance of the design was easily verified using the Agilent 89600 Vector Signal Analyzer software application. The output of the VHDL simulation was compared with the output of the system simulator. After conversion from VHDL into a FPGA the design was analyzed again with the same Vector Signal Analyzer.

The measured performance of the digital modulator is seen in Figure 4. The lower left screen shows the resulting spectral performance while the quality of the digitally constructed QPSK signal can be read from the EVM figure shown in the lower right of Figure 4 which indicates a value better than 0.9 %. The final design fits in a 100k gate FPGA.

### QPSK Demodulator

The second example is the implementation of a wideband QPSK receiver on a low cost reconfigurable hardware platform, see Figure 6. The resulting hardware is shown in Figure 5. The implementation is based on a combination of dedi-

Figure 4: Measured performance of the digital QPSK modulator

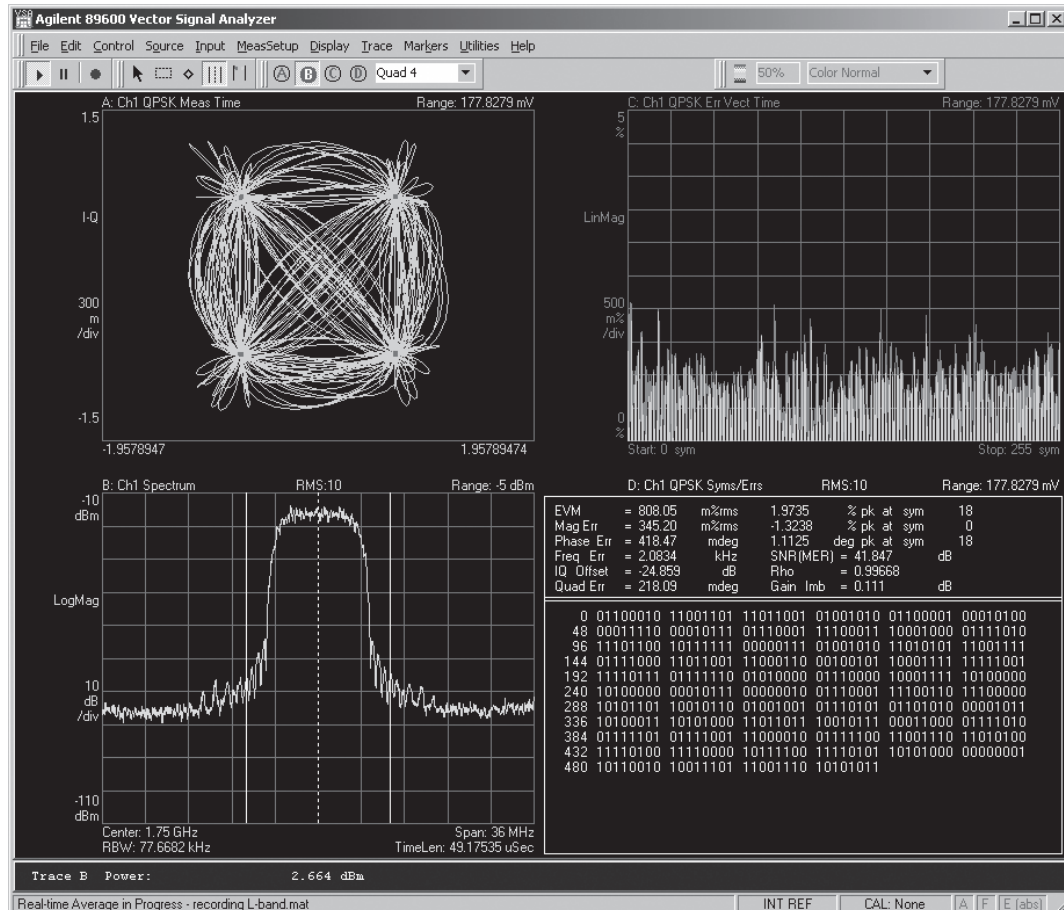




Figure 5: Reconfigurable Digital Receiver platform

cated ASIC's, FPGAs and a General Purpose Processor.

The receiver is equipped with a 12 bit A-to-D converter and a dedicated digital downconverter (DDC) chip from Analog Devices. This dedicated ASIC (AD6620) is chosen because a DDC is one of the generic blocks found in almost every digital receiver and it saves FPGA resources.

An analog front-end is needed in order to convert the high input frequency to a lower IF frequency. This IF is fed to the A-to-D converter which interfaces with the AD6620 digital downconverter. The digital downconverter is fully configurable via the general purpose processor (GPP). The platform is running on a single clock of 60 MHz. Hence a mechanism is needed for proper synchronization with the received input signal. The interleaved I and Q samples from the digital down converter are fed to FPGA 1 that performs the symbol timing

recovery loop and the carrier synchronization loop. FPGA 2 performs Forward Error Correction decoding.

The symbol timing recovery loop is one of the main blocks of a digital receiver. The design of this loop required a careful design cycle which resulted in extensive testing of every subpart in order to achieve the "one time right" implementation. In Figure 7 some major screenshots of the different levels of the design cycle are shown.

The upper left of Figure 7 shows the controlling behaviour of the quantized I and Q signals and the response of the loop on a large timing error at the input. The lower left presents a screenshot that shows the simulation of the VHDL model where the design was tested with the real-world test vectors. In the lower left the received signal constellation is shown where timing synchronization has been achieved. The constellation is rotated because carrier lock has to be performed after this block.

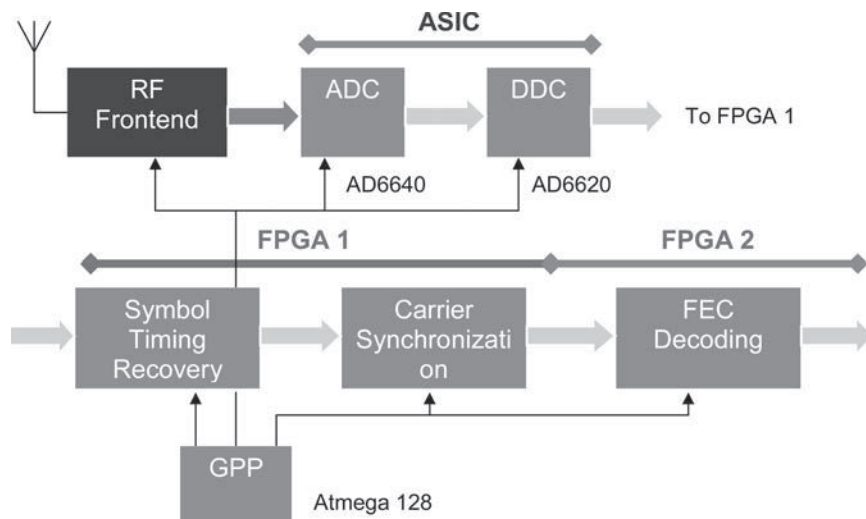
### SDR system examples

Some SDR system examples designed and developed by TNO are given. The focus is on the added value of SDR for the application rather than on the underlying technology.

### PESMO

PESMO is the Dutch acronym for the "Precision ESM receiver" which is the first system application example described here. "ESM" stands for Electronic Support Measures, and stands for the gathering of information by listening to radar and communication transmitters.

Figure 6 Digital demodulator



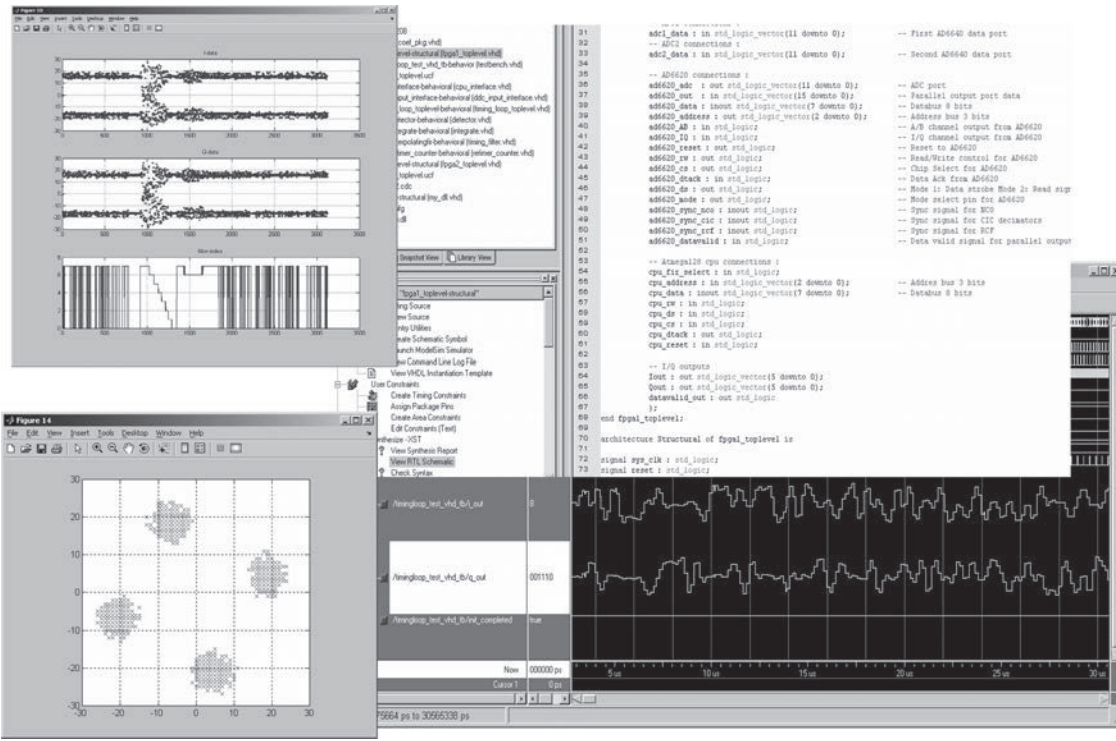


Figure 7: Results of various levels of simulation.

The precision ESM receiver is developed by TNO. The receiver is based on SDR technology which enables virtually any ESM algorithm to be used. The most common algorithms are listed:

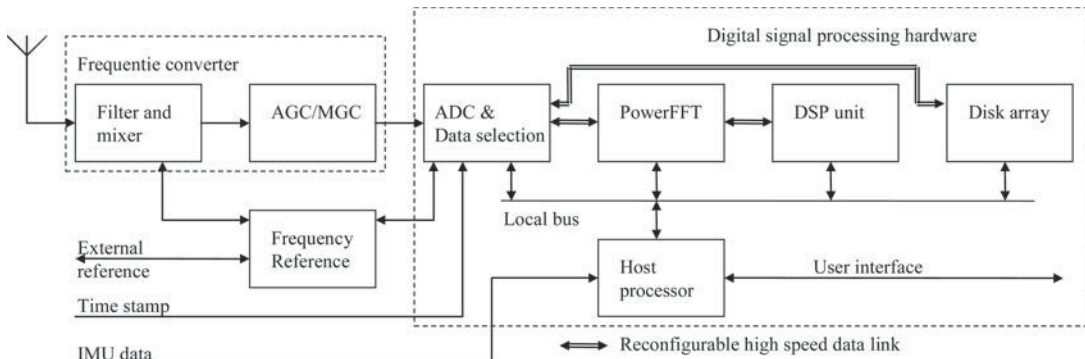
- Transmitter localization.  
Many algorithms are available for transmitter localization; TNO uses an algorithm based on frequency analysis.
- ELINT or Electronic Intelligence.  
The received signals are samples with high resolution and analyzed in detail afterwards.
- Advanced transmitter identification.  
The received signal is measured and compared to those in a database.

Transmitter localization was used as "example algorithm" to evaluate the SDR concept of the precision ESM receiver. The example algorithm is optimized to use from an aircraft, to allow for the tracking and tracing of transmitters.

Apart from this first frequency conversion stage, the receiver operates completely in the digital domain and is based on modern Software Defined Radio technology. The architecture of the receiver is given in Figure 8. Note that the high speed data links are shown in the configuration for passive emitter location and that they can be reconfigured to adapt the receiver to virtually any ESM application.

The converter adapts signal strength and frequency band of the received signal to that of the

Figure 8: Precision ESM receiver architecture



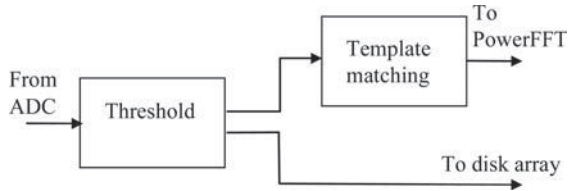


Figure 9: Data selection

Analogue to Digital converter (ADC). Any 500 MHz wide band between 100 kHz and 22 GHz can be converted to a fixed frequency of 500-1000 MHz.

The ADC and data selection block is an SDR based receiver for the actual radar of interest. The received data is sampled with 1 Giga samples/s and 8 bits resolution allowing for a real-time bandwidth of 500 MHz. The samples are combined in blocks of 1 kByte and passed to the data selection block. Data selection is performed fully in reconfigurable logic and is given in more detail in Figure 9. The first step is the application of a threshold preventing noise to be recorded. Only data exceeding a given threshold is passed. The application of a threshold effectively reduces the amount of data and hence data rate. All data exceeding the threshold is passed to the hard disk and recorded for optional off-line processing. The disk has a maximum transfer rate of 180 Mbyte/sec and a storage capacity of 500 GByte.

The template matcher can be optimized for the transmitter under surveillance, here SDR shows its real advantage since it allows adaptation to virtually any transmitter. The powerFFT and DSP are extensively used to analyze and interpret the received signal. This powerful signal processing chain allows for implementation of real-time ESM algorithms. The SDR based real-time processing chain and data link are fully programmable and reconfigurable.

The hardware of the receiver consists of Commercial Of The Shelf (COTS) hardware of EONIC, which allows for the receiver to be produced in series. The hardware components are shown in Figure 10.

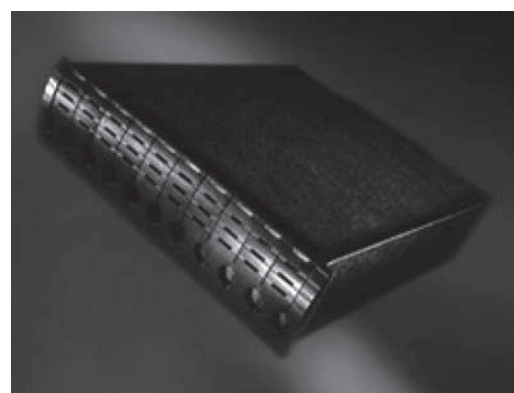
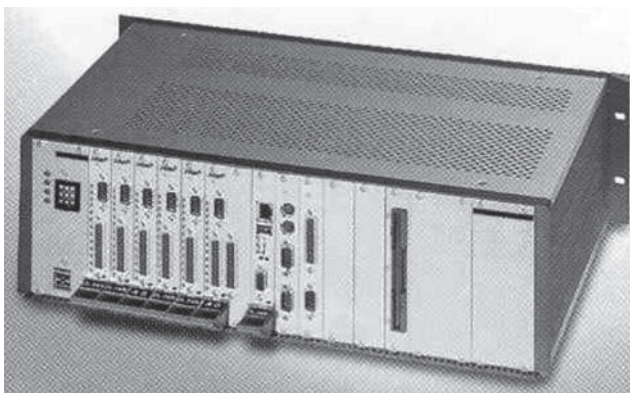
## ROCES

ROCES is the Dutch acronym for the "RealTime communication ESM receiver" which is the second system application example described here. The "real-time communication ESM receiver" is the communication equivalent of the radar oriented "Precision ESM receiver". The concept of the receiver is direction finding, a rather basic function. Due to the application of SDR technology, direction finding technology has made a major step forward. Direction finding is possible for up to 8 transmitters operating simultaneously at exactly the same frequency. More simultaneous transmitters can be separated when more antennas are used. Note: the "8" in the diagram notes the number of channels.

The signals are fed through an analog front-end and fed to a 14 bit A-to-D converter where each incoming channel is sampled with 30 Mega sample per second, where each sample is 2 byte. The data from the ADC can be stored to disk, resulting in an exceptionally large data rate of 480 Mbyte/s. The ADC data is also fed to the digital down converter where the bandwidth is reduced to 1 MHz. Digital down conversion results in a data rate of 128 Mega-byte per second. Also at this point data can be stored to disk.

The data of the digital down converter is fed to a so-called power storage box that includes a SDR based receiver for the signal under investigation. The SDR receiver prepares well defined batches of data (segments) that are processed by the general

Figure 10: EONIC digital processing hardware (left) and disk array (right)



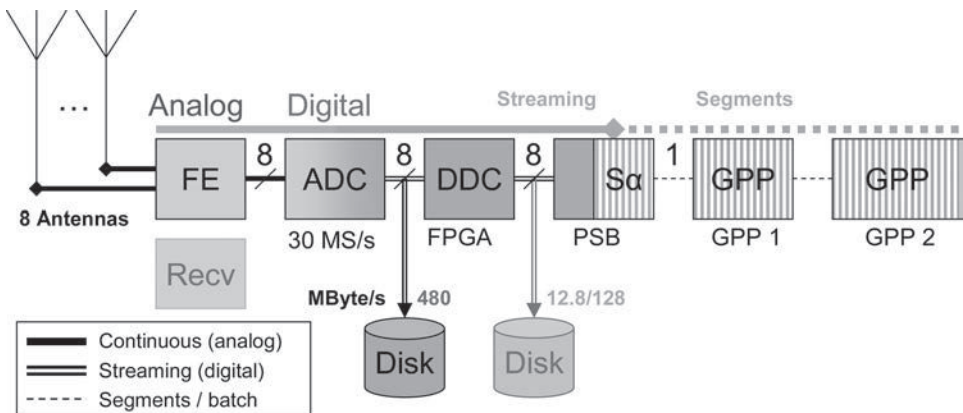


Figure 11: ROCES receiver architecture

purpose processors. Only a fraction of all segments is processed, resulting in an direction indication update about every second. Update rate of the direction finding algorithm can be increased by increasing the number of GPP. A variety of algorithms can be used on the GPPs, not only direction finding algorithms.

Given the operational context of direction finding (tracking moving vehicles and moving people), an update rate of about one second is fully adequate. Real time direction information is also used for further analysis of the data stored on disk.

## Conclusions

It can be concluded from the previous that software defined radio is a very attractive technology which

allows us to implement various radio systems and standards in reconfigurable platforms. It is shown that SDR technology is feasible, although it requires signal processing at a lower IF in most cases.

SDR technology can be used for a wide range of applications, from complex transmitter localization which uses adaptive beamforming techniques up to commercial digital communication systems.

Various digital hardware components can be used for implementing software radio hardware where the FPGA is one of the favourable components given its ability to perform high speed signal processing and easy reconfigurability.

# Channelizer

## The heart of ESM, ECM and SDR

van der Hoek  
info.request@eonic.com

### EONIC channelizer

Electronic Support Measures (ESM), Electronic Counter Measures (ECM), Electronic Warfare (EW) and Software Defined Radio (SDR) comprise the interception and analysis of radio signals from often unknown sources. Key questions which need to be answered are about the source of the signal (friend or foe) and the location of the transmitter. The key to answering these questions is by determining the protocols, coding and waveforms, as well as the locations of the radio stations and other information about the source. This is done by a channelizer. A channelizer extracts channels from the received RF-band for follow-on baseband processing, and, in the case of SDR, also inserts channels into the RF band for transmission.

Typically, the architecture of a channelizer consists of an analog front-end, which captures the signal from the radio spectrum. Subsequently, this signal is digitized and processed. User specific algorithms may be applied in a final step to distill the relevant information from the abundance of data captured at the front end.

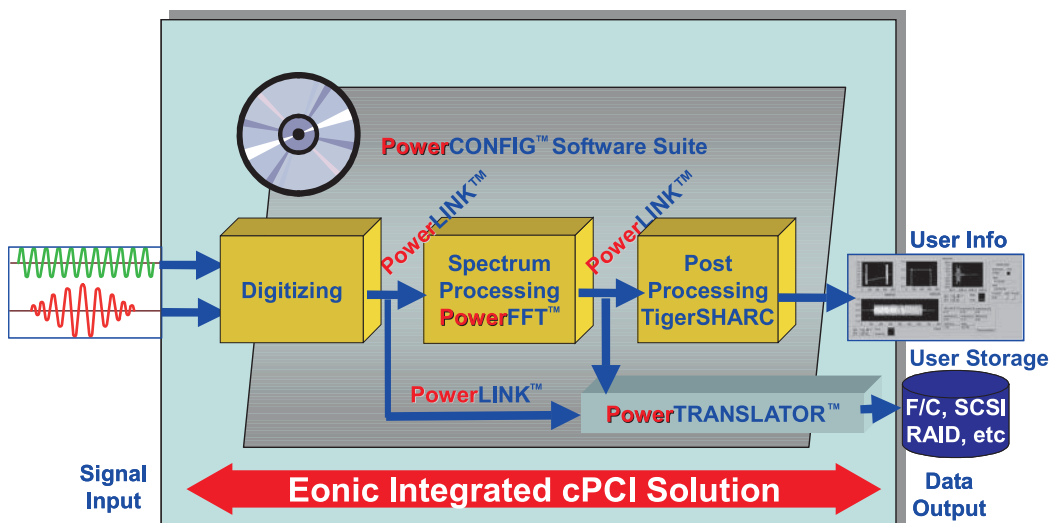
Figure 1: High Level System Architecture of a Channelizer. Analog inputs are digitized and offered for spectrum processing. Here, for example, channelization techniques like Digital Down Conversion, Frequency Domain Filtering, and Polyphase FFT Filter Banks can be deployed. Post processing is optional, as is writing the captured data to a storage device.

Typically, real-time front-end signal processing operations occur directly behind the digitizer and involve signal enhancement, polyphase filtering, spectrum analysis and synthesis as well as other functions. At the same time, digitizer technology advances towards broader bandwidths and higher resolutions allowing full digital IF/RF signal processing. Commonly available are 100 MHz at 14 bit ADC components, but newer components already digitize up to 400 MHz signals at 14 bit. The challenge hereby is to process the full digital bandwidth with sustained rate utilizing multi-mode, reconfigurable and flexible devices.

Current solutions for such real-time front-end processing are:

- Parallel DSP computing;
- FPGA based hardware.

Both processing solutions have many drawbacks. Parallel DSP computers are bulky and the power consumption is proportionally high. They require a



substantial software engineering effort for optimal code implementation.

FPGA based solutions may be smaller, typically a single board containing a few FPGAs and some memory components. However, for extreme processing requirements FPGAs become rigid solutions as the processing capability of FPGAs is often inversely proportional to the amount of flexibility. Another drawback is the high power consumption for FPGAs operating on such high data rates.

Eonic has therefore created a channelizer platform whereby the spectrum processing is performed by the PowerFFT™. This ASIC is used for massive FFT operations, in addition to FPGA-based reconfigurable computing and parallel DSP computing architectures. The key advantages this architecture is lower power consumption, much smaller footprint, lower costs and higher performance. This opens up a new generation of portable SDR and man-mounted ESM systems.

The benefits of this approach are obvious: whilst maintaining the benefits of reconfigurability, Eonic has opened up the road towards lightweight, smaller systems, which consume less power (and thus also generate less heat). These systems provide unparalleled performance and can be easily adapted to user-specific requirements.

### Systems Approach

The Channelizer provides a complete and portable system which isolates multiple channels in the wideband spectrum and presents the data for analysis in real-time. The system is housed in a 3U compactPCI enclosure. The system is extremely



versatile because of the many parameters which can be set by the user. The Channelizer can deploy a polyphase FFT filter bank, which is the most efficient way of channelization because it assumes redundancy within the frequency of the wideband channel. The filter bank isolates and decimates the various channels and then employs an FFT to efficiently convert each channel to baseband.

A number of options are available, which add to the uniqueness of Eonic's channelizer. The system is highly scalable to support multiple 105 MHz digitizers, maintaining real-time channelizing. It can also be expanded with expansion boards for additional programmeable logic, through Altera Stratix II FPGA boards, or enhanced real-time analysis with TigerSharc DSP boards. Furthermore, the Channelizer can be expanded into a very nimble SDR system by adding the transmit functionality with a DAC board.

### More information

Eonic BV

[www.eonic.com](http://www.eonic.com)

+31.15.260.0432

Delfttechpark 26

2628 XN Delft

The Netherlands

Email: More Information

Eonic BV ([www.eonic.com](http://www.eonic.com)), phone +31.15.260.0432

Delfttechpark 26, 2628 XH Delft, The Netherlands

Email: [info.request@eonic.com](mailto:info.request@eonic.com)

Fax: +31.15.260.0431

Eonic is an innovative supplier of reconfigurable solutions to the Defence and Security industry, providing real-time digitizing and signal processing platforms which are small, lightweight and power efficient. Eonic utilizes commercial off-the-shelf ASIC, FPGA and DSP technology in combination with advanced system engineering practices. Our systems are easily reconfigurable, scalable and flexible, providing an excellent platform for many types of applications. Eonic's systems are deployed in Radar, Sonar, Synthetic Aperture Radar, Electronic Warfare, Data Acquisition and Recording, Streaming Image Processing and other purposes.

Eonic - Digitally Mastering the Spectrum

# Software-Defined Radio Testbed for the Physical Layer of Wireless LANs

R. Schiphorst, N.A. Moseley and C.H. Slump  
Email: {r, schiphorst, n, a.moseley, c.h.slump}@utwente.nl

## Abstract

This paper presents a software-defined radio testbed for the physical layer of wireless LAN standards. All baseband physical layer functions have been successfully mapped on a Pentium 4 processor that performs these functions in real-time. This has been tested in combination with a CMOS integrated wideband analog front-end containing a low noise amplifier, down conversion mixers and filters.

The testbed consists of both a transmitter and a receiver. The transmitter contains a PC with a DAC board, an Agilent E4438C generator for upconversion and an antenna. The receiver consists of an antenna, a wideband analog front-end and a PC with an ADC board.

On this testbed we have implemented two different types of standards, a continuous-phase-modulation based standard, Bluetooth in the 2.4 GHz band and an OFDM based standard, HiperLAN/2 in the 5 GHz band. However, as all baseband processing is performed by software, our testbed can easily be extended to other standards.

To validate the SDR testbed we describe RF experiments for both Bluetooth and HiperLAN/2. In HiperLAN/2 mode, some sub-carriers are more noisy than others which is probably introduced by non-linearities in the analog frontend for example, non-linearities in the power amplifier. To investigate this effect, we have performed simulations in HiperLAN/2 mode to study these effects.

## Introduction

New wireless communications standards do not replace old ones, instead the number of standards keeps on increasing and by now an abundance of standards already exists, see Table I. Moreover, there is no reason to assume that this trend will ever stop. Therefore the software-radio concept is emerging as a potential pragmatic solution: a soft-

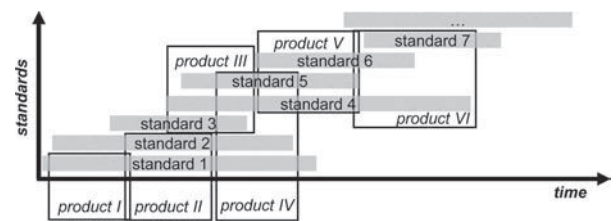
ware implementation of the user terminal able to dynamically adapt to the radio environment in which the terminal is located [1], [2].

Because of the analog nature of the air interface, a software radio will always have an analog front end. In an ideal software radio, the analog-to-digital converter (ADC) and the digital-to-analog converter (DAC) are positioned directly after the antenna. Such an implementation is not feasible due to the power that such device would consume and other physical limitations [3] [4]. It is therefore a challenge to design a system that preserves most properties of the ideal software radio while being realizable with current-day technology. Such a system is called a software-defined radio (SDR).

Software-defined radio has both advantages for consumers and manufacturers because current products support only a fixed number of standards. Figure 1 shows the lifetime of products and wireless standards. One can see that current-day products support a fixed number of standards and in time new standards emerge and old ones disappear, making a product eventually obsolete.

Software-defined radios on the other hand will enable consumers to upgrade their radio with new functionality e.g. required by new standards, just by software updates, without the need for new hardware. Moreover, manufacturers can upgrade,

Fig. 1: Standards support by products in time



patch or improve functionality of consumer-owned products and SDR could result in shorter development time, cheaper production due to less components. However, an important drawback of SDR is an increased power consumption, as dedicated designs are more power efficient. Especially for mobile applications, power consumption is very important.

First, this paper discusses the software-defined radio project at our university. Then, the built testbed is described including the results of some RF experiments. Finally, the use of non-linear power amplifiers in the transmitter is analyzed.

## Software-defined radio

Figure 2 depicts the mapping of the different functions as structure by the OSI model on software/hardware in current radio designs. The physical layer is generally implemented in hardware and higher layers are often software based with the Logical Link Control (LLC) and Medium Access Control (MAC) layer as transition area. In our first SDR project [5] we have researched whether the lowest layer of the receiver, the physical layer of wireless standards can be implemented in software running on a general purpose processor and estimate the costs of such an implementation with respect to power consumption and computational power requirements.

Thus, we interpret SDR as an implementation technology which differs from the views in [2] and [6]: flexible, universal, radio systems at each layer of the OSI model where manufacturers, network operators and consumer can benefit. Our interpretation on SDR is more focussed on the physical layer; an implementation technology, invisible for consumers. Moreover, we want to investigate if we can use existing processing capabilities (for example a notebook's CPU) for digital signal processing purposes thereby possibly prolonging the lifetime of a device. Moreover, it saves hardware and Moore's law will lower in time the computational load as a percentage of the computational capacity.

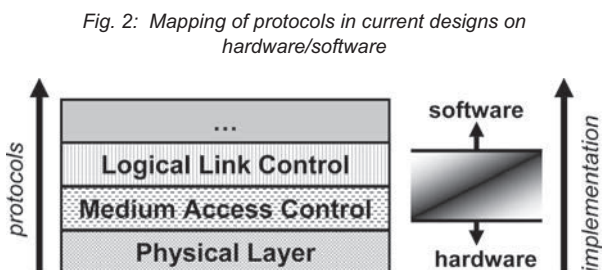


Fig. 2: Mapping of protocols in current designs on hardware/software

A flexible, all standard radio will always consume more energy than a dedicated radio, thus the first application for a flexible radio will be an application where power consumption is less an issue; an example being a flexible radio in a notebook. This application for SDR has three advantages. First, we can use the processing capabilities of the general purpose processor for digital signal processing purposes. Second, in comparison to SDR for mobile phones, our application can consume much more

Table I: Overview of wireless standards

Standard	Frequency band	Modulation type
CT2	864/868 MHz	GFSK
[1] CT2+	944/948 MHz	GFSK
DECT	1880-1900 MHz	GFSK
PHS	1893-1920 MHz	DQPSK
IEEE 802.15.4	2402 - 2480 MHz (N. America)	GFSK
	2412 - 2472 MHz (Europe)	
	2483 MHz (Japan)	
Bluetooth	2402 - 2480 MHz (N. America & Europe)	GFSK
	2447 - 2473 MHz (Spain)	
	2448 - 2482 MHz (France)	
	2473 - 2495 MHz (Japan)	
HomeRF	2402 - 2480 MHz (N. America & Europe)	GFSK
	2447 - 2473 MHz (Spain)	
	2448 - 2482 MHz (France)	
	2473 - 2495 MHz (Japan)	
IEEE 802.11a	5150 - 5250 MHz (USA)	OFDM: 2/4/16/64 QAM
	5250 - 5350 MHz (USA)	
	5725 - 5825 MHz (USA)	
IEEE 802.11b	2410 - 2462 MHz (N. America)	GFSK/DBPSK/DQPSK/QPSK
	2412 - 2472 MHz (Europe)	
	2483 MHz (Japan)	
HiperLAN/2	5150 - 5250 MHz (USA)	OFDM: 2/4/16/64 QAM
	5250 - 5350 MHz (USA)	
	5725 - 5825 MHz (USA)	
	5150 - 5350 MHz (Europe)	
	5470 - 5725 MHz (Europe)	
	5725 - 5875 MHz (Europe)	
	5150 - 5250 MHz (Japan)	
IS-54/IS-136	824 - 849 MHz	CDMA: π/4 DQPSK
	869 - 894 MHz	
	1850 - 1910 MHz	
	1930 - 1990 MHz	
IS-95	824 - 849 MHz	CDMA: QPSK/OQPSK
	869 - 894 MHz	
	1850 - 1910 MHz	
	1930 - 1990 MHz	
	1920 - 1980 MHz (Asia only)	
IMT-2000/UMTS	2110 - 2170 MHz (Asia only)	
	1920 - 1980 MHz	
	2110 - 2170 MHz	
	1900 - 1920 MHz	
	2010 - 2025 MHz	
GSM	824 - 849 MHz	GMSK
	869 - 894 MHz	
	880 - 915 MHz	
	925 - 960 MHz	
	1710 - 1785 MHz	
	1805 - 1880 MHz	
	1850 - 1910 MHz	
	1930 - 1990 MHz	
PDC	810 - 826 MHz	π/4 DQPSK
	940 - 956 MHz	
	1429 - 1441 MHz	
	1453 - 1465 MHz	
	1477 - 1489 MHz	

power (in the order of 1 W). Third, a notebook is very suited for demonstration purposes.

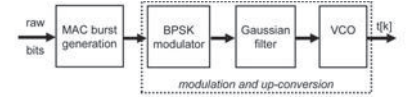
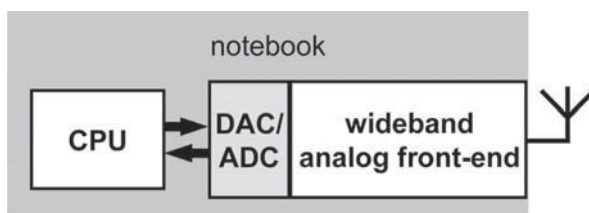
Table I gives an overview of important wireless standards together with the used frequency bands and modulation type. It seems that each standard can be seen as a family of standards, an example being GSM. Thus the number of existing standards that manufacturers have to support is even larger than one would initially expect. However, there are also similarities among them: the used frequency bands are between 0.8 and 6 GHz with dominant frequency bands around the 0.8 GHz, 2 GHz, 2.4 GHz and 5 GHz.

In our SDR research we decided not to focus on an allstandard radio but to start with a software-defined radio for wireless LAN standards first. At the project's start we defined also the scope of project: the physical layer of the OSI model. Recent literature [7] indicates however that especially error correction decoding (Viterbi algorithm) requires most computational power in the lower layers of a system. Figure 3 summarizes the design goal of our project, a notebook with a wideband RF frontend with a software implementation of the physical layer.

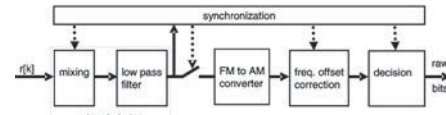
Wireless LAN standards use phase modulation or OFDM (Orthogonal Frequency Division Multiplexing) in the 2.4 GHz or 5 GHz frequency band, so we decided in our project to combine an instance of a continuousphase modulation standard (Bluetooth) with an OFDM standard (HiperLAN/2).

HiperLAN/2 [8] is a high-speed Wireless LAN (WLAN) standard using OFDM. Its physical layer is very similar to the 802.11a standard. Bluetooth [9] on the other hand is a low cost, low speed standard, designed for replacing fixed cables. Bluetooth uses Gaussian Frequency Shift Keying (GFSK) which is also used by other standards such as HomeRF and DECT.

*Fig. 3: Project scope*



(a) Bluetooth transmitter



(b) Bluetooth receiver

*Fig. 4: Functional architecture of the Bluetooth transmitter and receiver*

## Testbed

### Functional architecture

For every implementation of an SDR transceiver, integration of both transceivers at a functional level is important. This section describes the functional architecture both of a CPM standard (Bluetooth) and an OFDM standard (HiperLAN/2). As we aimed in our first SDR project at the receiver side, the end of this section discusses only the functional architecture of a Bluetoothenabled HiperLAN/2 receiver.

### Bluetooth

Figure 4 depicts the functional architecture of the Bluetooth transmitter and receiver in our testbed. The first step in the transmitter is to embed the raw bits into MAC bursts which are then BPSK modulated at 1 Mbit/s. The BPSK symbols are filtered by a Gaussian low pass filter and the filtered output is connected to an VCO that translates the amplitude variation into frequency variations. At the receiver side, the first step is to select the wanted Bluetooth channel and suppressing all others which is performed both digitally and by the analog front-end. This is achieved by mixing the wanted channel to zero IF and applying a low-pass filter. The next step is to demodulate the FM signal into an AM signal by taking the derivative of the phase. Because an frequency offset introduces an offset in the AM signal, it has to be corrected before bit decision.

### HiperLAN/2

Figure 5 depicts the HiperLAN/2 physical layer architecture which is very different from the Bluetooth architecture one. The HiperLAN/2 transmitter starts with mapping raw bits on QAM symbols (either BPSK, QPSK, 16-QAM or 64-QAM symbols). In the next step, the QAM symbols are mapped on data carriers and an OFDM symbol is constructed by adding pilot carriers, applying an inverse FFT and adding an prefix, which results in

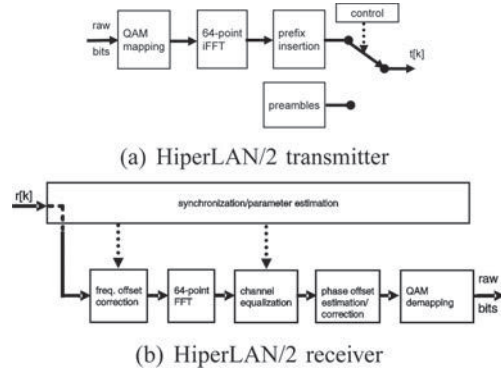


Fig. 5: Functional architecture of the HiperLAN/2 transmitter and receiver

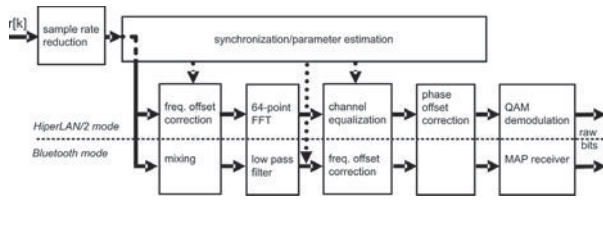
a 20 MSPS signal. MAC bursts are then created by adding special symbols, preambles, to the start of the MAC burst.

The HiperLAN/2 receiver starts by searching for the start of a MAC burst. If found, it estimates the frequency offset and channel parameters. After these steps the data OFDM symbols can be demodulated by first correcting the frequency offset, performing an FFT, correcting the channel and detecting and correcting the phase offset by using the pilot tones. The output consists of QAM symbols which have to be de-mapped into raw bits.

### Functional architecture of a Bluetooth-enabled HiperLAN/2 receiver

Although the functional architecture of both standards is very different, we have successfully integrated the functional architecture of the Bluetooth receiver into the HiperLAN/2 receiver [10] by using a (simplified) maximum a posteriori probability (MAP) receiver which is a more advanced Bluetooth demodulation algorithm [1]. In this testbed, however, we did not implement this receiver (yet) but used instead a conventional receiver such as depicted in Figure 4.

Fig. 6: Functional architecture of the Bluetooth-enabled HiperLAN/2 receiver



<sup>1</sup> We use a non-real time operating system, e.g. linux and therefore the transmitter and receiver programs use large buffers of 100 ms to avoid the influence of the operating system.

### Testbed setup

Figure 7 shows the component architecture of our SDR testbed. The testbed consists of eight components; a transmitter PC, a DAC PC board, an Agilent E4438C generator, two antennas, a wideband SDR analog frontend, a receiver PC and an ADC PC board.

The transmitter PC continuously generates HiperLAN/2 or Bluetooth MAC bursts which are sent in realtime<sup>1</sup> to the DAC board at 20 MSPS by using an Adlink cPCI-7300 digital I/O PCI card. This DAC board converts the digital signal into a complex analog baseband signal which is upconverted to radio frequencies by the Agilent E4438C generator. This RF signal is transmitted through the air and received by the receiver antenna. The antenna output is connected to the wideband SDR analog front-end that converts the RF signal into a baseband signal. The ADC board samples this analog signal with 80 MSPS and the onboard Intersil ISL5416 programmable down converter

Fig. 7: Component architecture of the SDR testbed

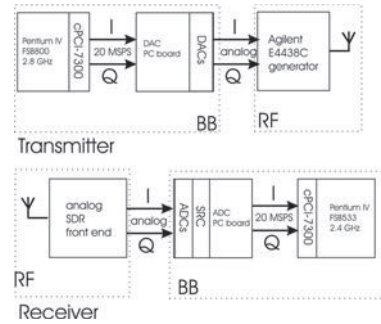
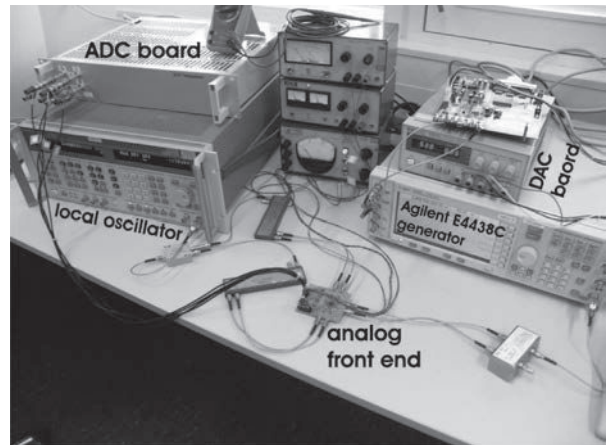


Fig. 8: Experiment setup (both computers are not shown)



(SRC) decimates the digital signal into a complex 20 MSPS signal in HiperLAN/2 mode and into a 5 MSPS signal (including mixing of the wanted channel to baseband) for Bluetooth. This signal is transported to the receiver PC by using another Adlink cPCI-7300 digital I/O PCI card. The receiver PC performs all demodulation functions and demodulates the MAC bursts real-time.

## Experiments

RF experiments have been performed with the setup of Figure 7 (without antennas) and a picture of the testbed is shown in Figure 8. In both Bluetooth and HiperLAN/2 mode, successful transmission and reception of continuously transmitted MAC bursts is achieved. In addition, some initial tests have been performed successfully with antennas in Bluetooth mode.

In Bluetooth mode, the receiver operates from -20.0 to -69. 4 dBm signal strength<sup>2</sup> within the specifications of the standards i.e. the BER is below 0. 1% . Figure 9 depicts the eye-diagram for both -20. 0 and -69. 4 dBm Bluetooth signal. The first eye-diagram

is very open whereas with the weak signal at -69. 4 dBm, the eyediagram is almost closed.

In HiperLAN/2 mode, the receiver works only for BPSK, QPSK and 16-QAM mode. In 64-QAM mode, the PER (Packet Error Rate) is always larger than 10% . Figure 10 shows the output of the channel estimation algorithm for the three lower modes of HiperLAN/2. It seems that the variations

*Fig. 10: RF experiments: Output of the HiperLAN/2 channel estimation algorithm. (A large bar indicates a large variation.)*

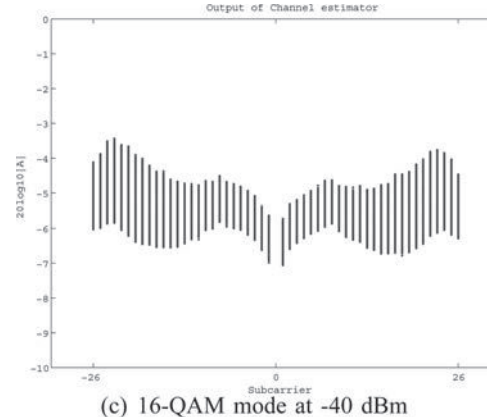
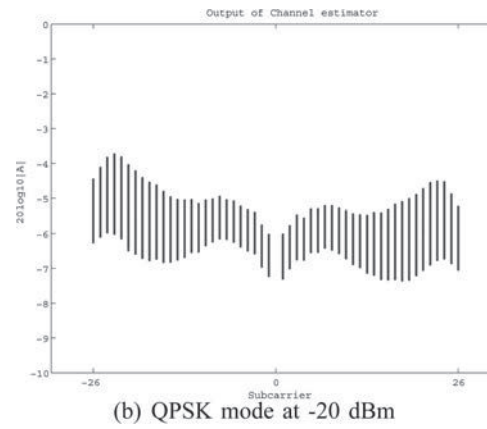
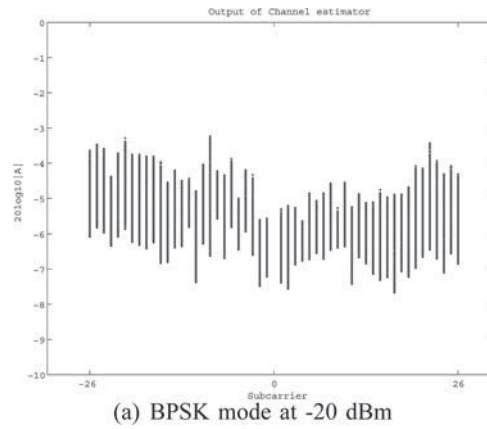
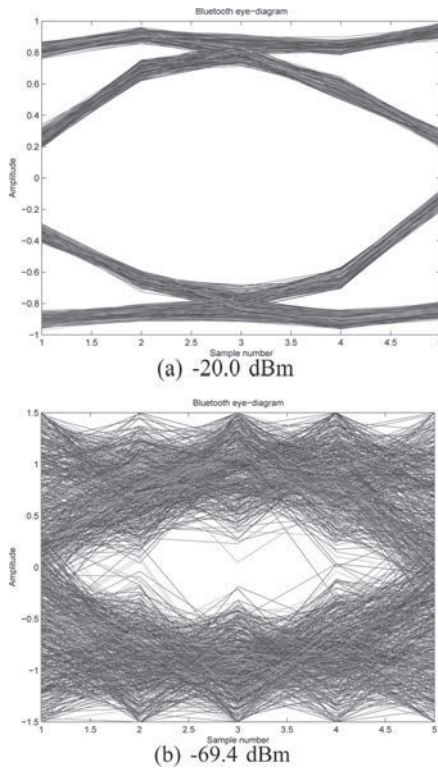


*Fig. 9: RF experiments: Eye-diagram of received Bluetooth signal.*



<sup>2</sup> We have calibrated the output of the Agilent generator by manually measuring the RMS value of the generator output.

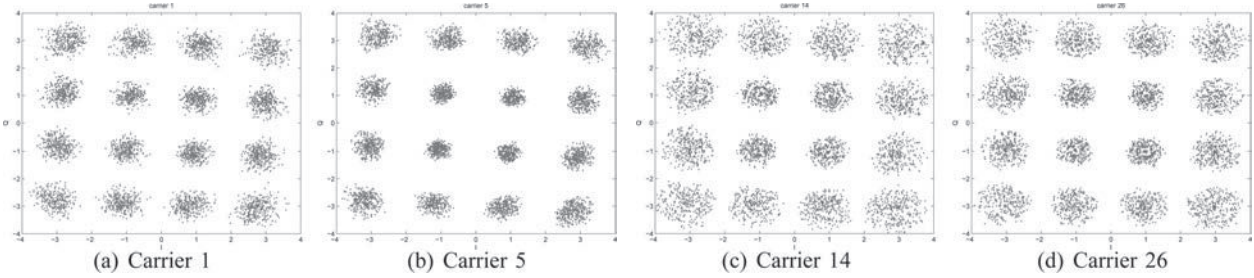


Fig. 11: RF experiments: 16-QAM constellation diagrams for several carriers at -40 dBm signal strength.

of the outer carriers is higher than for lower carriers.

Figure 11 depicts for the constellation of several carriers in 16-QAM mode. It seems that for all carriers, the constellation points at the border of the constellation diagrams are more noisy than the inner points. Additional research is necessary to identify the causes of the worse performance in HiperLAN/2 mode. One of the possible causes for this could be non-linear power amplifiers in the transmitter.

### Non-linear power amplifiers

In OFDM systems the power amplifier (PA) in the transmitter has a large impact on the performance of the system. Real-world OFDM power amplifiers are weakly non-linear. This causes intermodulation between OFDM sub-carriers.

The effect of this intermodulation is two-fold. Firstly, some intermodulation products are outside the channel causing interference to adjacent channels. Filtering at the output of the PA can reduce these unwanted spurious responses. Secondly, the remaining products are located inside the channel. This causes self-interference and raises the bit-error rate.

The amount of intermodulation caused by the PA depends on the drive level. Reducing the drive level of the amplifier is called *backoff*. The amount

of backoff is specified in dB referenced to the 1 dB compression point of the PA.

Simulations were performed of a non-linear PA model in combination with the HiperLAN/2 software developed in the SDR project.

### PA simulation setup

We incorporated the non-linear baseband-equivalent PA model from 'example 1' [11] into our HiperLAN/2 software. A block diagram of the simulation setup is shown in Figure 12.

We extended the PA model to include a saturation region. This was needed because the original PA model breaks down beyond a certain input level. In Figure 13 the power characteristics of the original and extended model are shown.

The extension of the model is achieved by reducing the input signal magnitude when the magnitude is beyond or at the saturation point of the PA.

The channel bit-error rate is calculated under different PA input backoff conditions and modulation schemes. The simulated backoff range is from -3 dB to 7 dB using BPSK, QPSK, QAM16 and QAM64 modulated sub-carriers. The number of transmitted bits is  $1 \cdot 10^6$  for each condition.

Fig. 13: Power characteristic of the PA model.

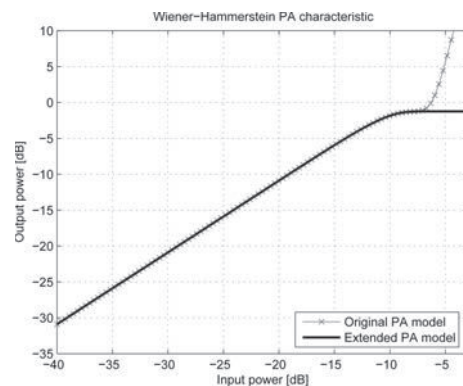
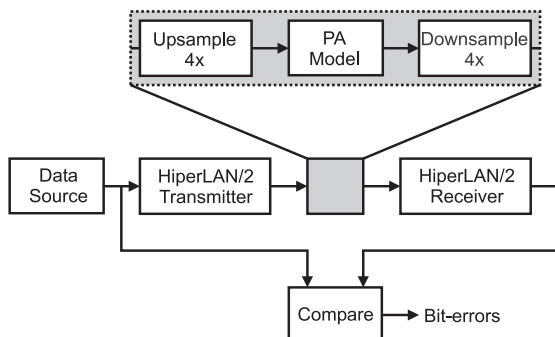


Fig 12: Non-linear PA simulation setup



## Results

A graph showing the channel bit-error rate plotted against PA backoff is shown in Figure 14. It is clear that the channel bit-error rate depends heavily on the sub-carrier modulation scheme. For BPSK and QPSK modulated sub-carriers, the bit-error rate introduced by the PA is below  $1 \cdot 10^{-4}$ <sup>3</sup> for backoff amounts over 0 dB. For QAM16, however, the bit-error rate drops below  $1 \cdot 10^{-4}$  for backoff amount larger than 5 dB.

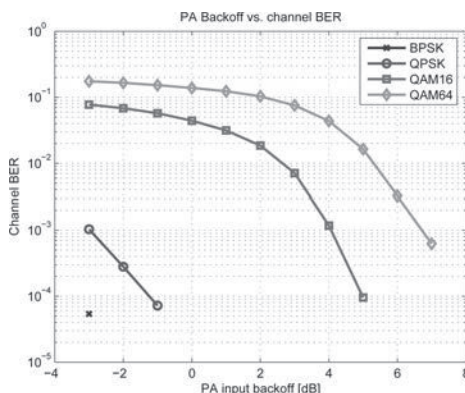
In Figure 15, 16 and 17 the constellation diagrams of carrier 26 are plotted under different modulation and PA backoff conditions.

The figures show well-defined constellations for BPSK and QPSK under all three simulated backoff conditions. This indicates that BPSK and QPSK modulated subcarriers are quite insensitive to weak PA non-linearities.

The constellation diagrams for QAM16 and QAM64 modulated sub-carriers show that considerable distortion takes place under low PA backoff conditions. In the QAM64 case, the constellation diagrams show clustering only for a PA backoff of 6 dB, while for QAM16 clustering is already recognizable at a PA backoff of 3 dB. These modulation schemes are clearly more sensitive to weak non-linearities.

The simulations show that the increased bit-error rate for QAM16 and QAM64 observed during experiments using the SDR testbed could be caused by non-linearities in the power amplifier of the transmitter. However, any non-linear component in the transmitter-receiver chain could cause the same distortion effects.

Fig. 14: Simulation results of channel BER against PA backoff.



<sup>3</sup> The HiperLAN/2 standard requires a BER (after error correction) below  $2 \cdot 10^{-4}$  [1]. So if the channel BER (before error correction) is lower than  $1 \cdot 10^{-4}$ , its influence on the system can be neglected.

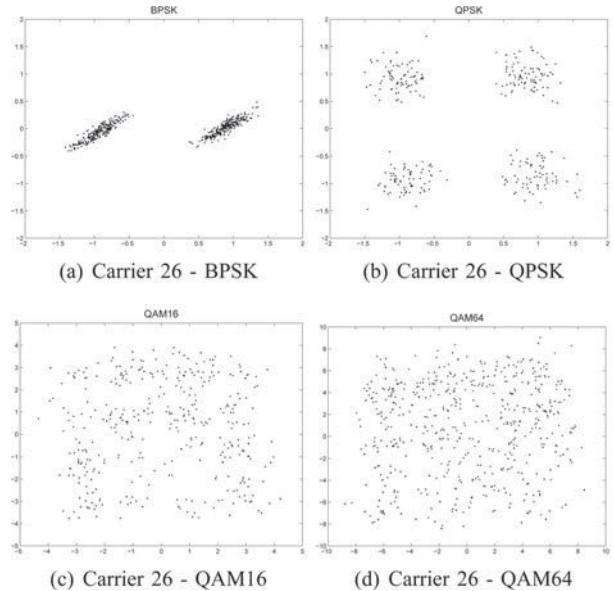


Fig. 15: Constellation diagrams for carrier 26 (PA backoff = 0 dB)

## Conclusions

In this paper we have presented a Software-Defined Radio testbed for wireless LAN standards. On this testbed we have implemented successfully two different types of standards, a continuous-phase-modulation based standard, Bluetooth and an OFDM based standard, HiperLAN/2. However, our testbed can easily be extended to other standards, because the only limitations in our testbed are the maximal channel bandwidth of 20 MHz, the dynamic range of the wideband SDR analog front-end and of course the processing capabilities of the PC.

In RF experiments with the testbed, we have seen that in HiperLAN/2 mode, some sub-carriers are more noisy than others. This is probably caused by non-linearities in the analog front-end. For that reason we have performed simulations in HiperLAN/2 mode with non-linear power amplifiers in the transmitter. Especially for higher modes i.e. QAM16 and QAM64, we have seen that a nonlinear amplifier has a large impact on the performance. However, by reducing the output power, this impact can be minimized to acceptable levels. For QAM64, the backoff has to be at least 6 dB. Digital pre-distortion algorithms could reduce this backoff factor.

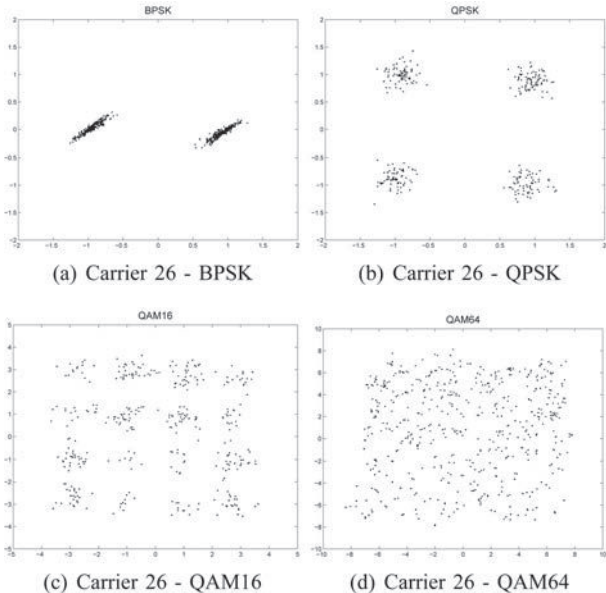


Fig. 16: Constellation diagrams for carrier 26 (PA backoff = 3 dB)

Further investigation is necessary to identify other sources of non-linearities in analog front-end (both transmitter and receiver) of the testbed.

## Acknowledgments

We thank our colleagues from the IC-Design group for their work on the analog part of the front-end and for interesting discussions. Moreover, we thank Henny Kuipers and Geert-Jan Laanstra for building the DAC and ADC board.

## References

- [1] R. Schiphorst. Software-Defined Radio for Wireless Local-Area Networks. PhD thesis, University of Twente, September 2004.
- [2] J. Mitola. Software Radio Architecture: Object-Oriented Approaches to Wireless Systems Engineering. Wiley, 2000.
- [3] R.H. Walden. Performance trends for analog-to-digital converters. IEEE Communications Magazine, pages 96-101, February 1999.
- [4] V.J. Arkesteijn, E.A.M. Klumperink, and B. Nauta. An Analogue Front-End Architecture for Software Defined Radio. 13th proRISC workshop, November 2002.
- [5] The Bluetooth-HiperLAN/2 SDR receiver project website. <http://www.sas.el.utwente.nl/home/SDR/>.
- [6] W. Tuttlebee. Software Defined Radio: Origins, Drivers and International Perspectives. John Wiley & Sons, 2002.
- [7] K. Masselos, S. Blionas, and T. Rautio. Reconfigurability requirements of wireless communication systems. IEEE heterogeneous

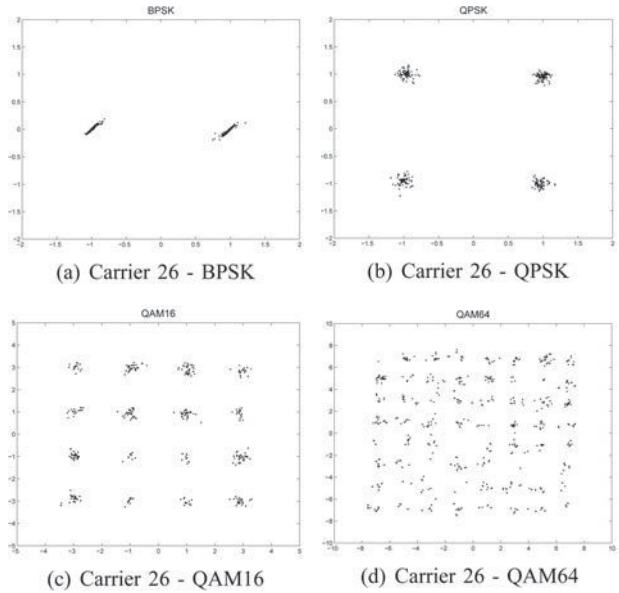


Fig. 17: Constellation diagrams for carrier 26 (PA backoff = 6 dB)

reconfigurable systems-on-chip workshop, 2004.

- [8] ETSI. Broadband Radio Access Networks (BRAN); HIPERLAN Type 2; Physical (PHY) layer. Technical Specification ETSI TS 101 475 V1.2.2 (2001-02), ETSI, February 2001.
- [9] Bluetooth SIG. Specification of the Bluetooth System - Core. Technical Specification Version 1.1, 'Bluetooth SIG', February 2001.
- [10] R. Schiphorst, F.W. Hoeksema, and C.H. Slump. Implementation alternatives for a flexible wireless LAN transceiver. Workshop on Software Radios (WSR2004), Karlsruhe (G), March 2004.
- [11] Lei Ding et al. A Robust Digital Baseband Predistorter Constructed Using Memory Polynomials. IEEE Transactions on Communications, January 2004.
- [12] <http://www.semiconductors.philips.com/comms>.

## Authors

R. Schiphorst, N.A. Moseley and C.H. Slump  
University of Twente, Department of Electrical  
Engineering, Mathematics and Computer Science  
(EEMCS), Signals and Systems group (SaS),  
P.O. box 217  
7500 AE Enschede - The Netherlands  
Phone: +31 53 489 2770  
Fax: +31 53 489 1060  
Email: {r, schiphorst, n, a.moseley, c.h.slump}@utwente.nl

# Spanningsversterking met weerstanden en condensatoren

Ir. H.C. Bleijerveld



Kan een schakeling die alleen weerstanden en condensatoren bevat een elektrische spanning versterken? Velen denken van niet, maakte ik op uit vragen aan diverse collega's.

Toch kan het! Bijvoorbeeld met de eenvoudige schakeling van figuur 2 die slechts vier componenten bevat.

Na enig rekenwerk volgt:

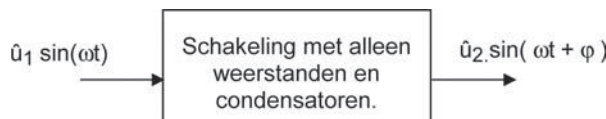
$$\frac{\hat{u}_2}{\hat{u}_1} = \sqrt{\frac{\omega^4 \tau^4 + 9 \omega^2 \tau^2}{\omega^4 \tau^4 + 7 \omega^2 \tau^2 + 1}}, \text{ met } \tau = RC.$$

Voor bepaalde hoekfrequenties  $\omega$  is  $\hat{u}_2 / \hat{u}_1$  groter één, zodat inderdaad sprake is van *spanningsversterking*. Figuur 3 illustreert dat.

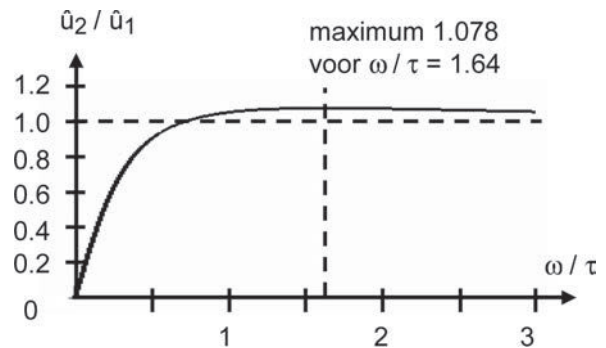
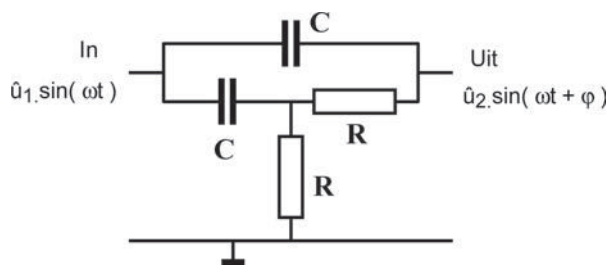
Voor wie het precies will weten: de spanningsversterking is maximaal

$$\frac{\sqrt{305-10\sqrt{19}}}{15} \approx 1.078 \text{ en treedt op voor}$$

Figuur 1: Kan  $\frac{\hat{u}_2}{\hat{u}_1} > 1$  zijn?



Figuur 2: Voor bepaalde  $\omega$  is  $\hat{u}_2/\hat{u}_1 > 1$



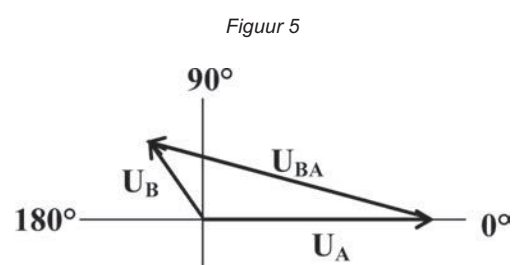
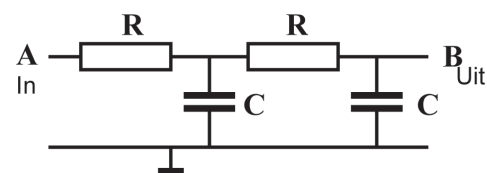
Figuur 3: De amplitude-overdrachtsfunctie van de schakeling van figuur 2.

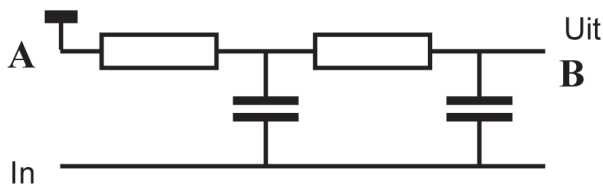
$$\omega = \frac{\sqrt{1+\sqrt{19}}}{\tau\sqrt{2}} \approx \frac{1.637}{\tau} \text{ rad/sec.}$$

## De achterliggende gedachte

De fasedraaiing van het laagdoorlaatfilter van figuur 4 loopt van nul voor lage frequenties, tot  $180^\circ$  voor hoge frequenties. Zodra de fasedraaiing meer is dan  $90^\circ$ , is de spanning tussen A en B groter dan de ingangsspanning. Het vectordiagram van figuur 5 illustreert dat.

Figuur 4: een eenvoudig laagdoorlaatfilter.





Figuur 6: Zelfde schakeling als figuur 2.

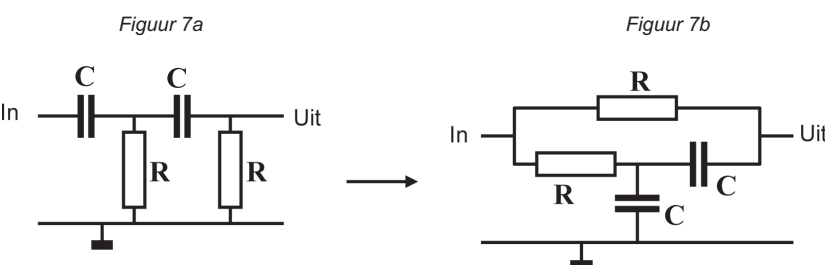
Door in figuur 4 punt A als massa te beschouwen en de massa als ingang, ontstaat figuur 6.

Voor bepaalde frequenties is de amplitude  $|U_{AB}|$  van de spanning op uitgang dus groter dan op de ingang. De tekenwijze van figuur 6 is ongebruikelijk. Het is echter dezelfde schakeling als die van figuur 2, alleen anders getekend!

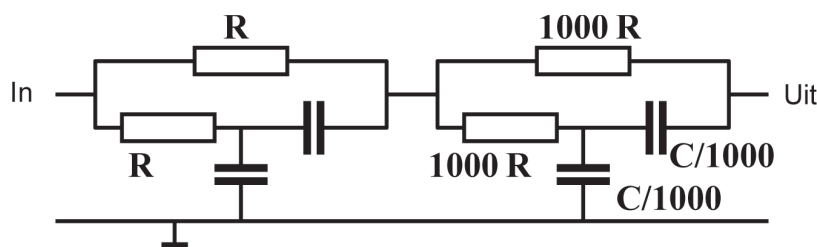
### Variant

Hetzelfde principe is mogelijk met het *hoogdoorlaat-filter* van figuur 7a, waaruit de schakeling van figuur 7b volgt. Ook hier is de maximale spanningsversterking 1.078. Deze treedt op bij een frequentie van ongeveer

$$\omega = \frac{0.611}{\tau}, \text{ met } \tau = RC.$$



Figuur 8: Schakeling met spanningsversterking van 1.16 voor wisselspanning van  $0.260/\tau$  Hz.



### Grotere spanningsversterking mogelijk?

Is een grotere spanningsversterking dan 1.078 mogelijk? Ja, door twee schakelingen van het type van figuur 2 in cascade te schakelen. Dat gaat alleen goed als de tweede trap de eerste niet te zwaar belast. Dat is mogelijk door de weerstanden in de tweede trap 1000 × zo groot te kiezen en capaciteiten evenveel keer zo klein. Aldus ontstaat de schakeling van figuur 8.

Uit een simulatieprogramma (ik gebruikte Microcap, waarvan een gratis demonstratieversie is te verkrijgen op [www.spectrum-soft.com](http://www.spectrum-soft.com)) volgt dat een spanningsversterking van ongeveer 1.16 haalbaar is voor hoekfrequentie  $1.63/\tau$  rad/sec ofwel  $0.260/\tau$  Hz.

# Ledenmutaties NERG



## Nieuwe leden:

Breur, ir. J.J.  
Boulevard Heuvelink 1-8,  
6828 KG ARNHEM  
Hezewijk, ir. J.G. van  
Loosduinsestraat 49,  
2729 CM ZOETERMEER  
Kroeze, dr. ing. H.  
Lorentzweg 175,  
1223 HP HILVERSUM  
Swaluw, ing. M.S.  
Schepenenstraat 24,  
3641 HP UITHOORN  
Tempelman, bc C.A.A.  
Dorpsplein 8,  
4443 AD NISSE

## Nieuwe adressen:

Alberts, ing. S.A.  
Klarinetstraat 57,  
1312 NE ALMERE  
Bolt, ir. R.J.  
Prinsengracht 50 A,  
2512 GA 'S-GRAVENHAGE  
Dijkhuis, ir. J.F.  
Tolhuis 1315,  
6537 MR NIJMEGEN  
Doggen, J.M.  
Albert Luthulistraat 28-A,  
1091 NW AMSTERDAM  
Huijs, ir. J.A.C.  
Artilleriestraat 18,  
7433 MN SCHALKHAAR  
Koole, ir. C.Th.  
Annadal 43,  
5513 XP VALKENSWAARD  
Mulder, ir. H.  
Steenbok 33,  
2221 PX KATWIJK (ZH)

Nieuwland, ing. P.M. van  
De Follingen 4,  
5581 AE 'WAALRE  
Schipper, ing. B.H.  
Hooftstraat 329, 2406  
GK ALPHEN A/D RIJN  
Schmidt, ir. J.R.  
Bastiaansplein 101,  
2611 DC DELFT  
Schramp, ir. R.  
Plesmanlaan 25,  
2497 CD DEN HAAG  
Steffen, W.  
Albert Luthulistraat 28-a,  
1091 NW AMSTERDAM  
Verweijen, ir. F.L.J.  
Vivaldistraat 117, 2901  
HE CAPELLE A/D IJSEL



## Herhaalde oproep voor leden van het NERG

Het bestuur van het NERG maakt u attent op de volgende vacatures:

**Ledenwervingsmanager**  
**Leden Programmacommissie**  
**Leden Redactiecommissie**

Indien u geïnteresseerd bent in één van deze vacatures, dan kunt u contact opnemen met het NERG via: [secretariaat@nerg.nl](mailto:secretariaat@nerg.nl)

**Het NERG heeft u nodig!**